Noninvasive Human Brain Stimulation

Timothy Wagner,[1] Antoni Valero-Cabre,[1,2,3] and Alvaro Pascual-Leone[1,4]

[1]Center for Noninvasive Brain Stimulation, Beth Israel Deaconess Medical Center, Department of Neurology, Harvard Medical School, Boston, Massachusetts 02215; email: apleone@bidmc.harvard.edu

[2]Laboratory of Cerebral Dynamics, Plasticity and Rehabilitation, Department of Anatomy and Neurobiology, Boston University School of Medicine, Boston, Massachusetts 02218

[3]LPNC, CNRS Unit 5105-ERT-Treat Vision, Department of Neurology, Fondation Ophtalmologique Rothschild, 75019 Paris, France

[4]Institut Guttmann d'Rehabilitacio, Universitat Autonoma, Barcelona, Spain

Annu. Rev. Biomed. Eng. 2007. 9:527–65

First published online as a Review in Advance on April 19, 2007

The *Annual Review of Biomedical Engineering* is online at bioeng.annualreviews.org

This article's doi: 10.1146/annurev.bioeng.9.061206.133100

1523-9829/07/0815-0527$20.00

Key Words

TMS, tDCS, electromagnetism, neural networks, modeling, neurophysiology, neuromodulation, therapeutic applications, rehabilitation

Abstract

Noninvasive brain stimulation with transcranial magnetic stimulation (TMS) or transcranial direct current stimulation (tDCS) is valuable in research and has potential therapeutic applications in cognitive neuroscience, neurophysiology, psychiatry, and neurology. TMS allows neurostimulation and neuromodulation, while tDCS is a purely neuromodulatory application. TMS and tDCS allow diagnostic and interventional neurophysiology applications, and focal neuropharmacology delivery. However, the physics and basic mechanisms of action remain incompletely explored. Following an overview of the history and current applications of noninvasive brain stimulation, we review stimulation device design principles, the electromagnetic and physical foundations of the techniques, and the current knowledge about the electrophysiologic basis of the effects. Finally, we discuss potential biomedical and electrical engineering developments that could lead to more effective stimulation devices, better suited for the specific applications.

Contents

INTRODUCTION

The past decade has seen a rapid increase in the application of noninvasive brain stimulation to study brain-behavior relations and treat a variety of neurologic and psychiatric disorders. Noninvasive brain stimulation provides a valuable tool for interventional neurophysiology applications, modulating brain activity in a specific, distributed, cortico-subcortical network so as to induce controlled and controllable manipulations in behavior; as well as for focal neuropharmacology delivery, through the release of neurotransmitters in specific neural networks and the induction of focal gene expression, that may yield a specific behavioral impact. Noninvasive brain stimulation is a promising treatment for a variety of medical conditions, and the number of applications continues to increase with the large number of ongoing clinical trials in a variety of diseases. Therapeutic utility of noninvasive brain stimulation has been claimed in the literature for psychiatric disorders, such as depression, acute mania, bipolar disorders, hallucinations, obsessions, schizophrenia, catatonia, post-traumatic stress disorder, or drug craving; neurologic diseases, such as Parkinson's disease, dystonia, tics, stuttering, tinnitus, spasticity, or epilepsy; rehabilitation of aphasia or of hand function after stroke; and pain syndromes, such as those caused by migraine, neuropathies, and low-back pain; or internal visceral diseases, such as

chronic pancreatitis or cancer. Even though such claims are insufficiently supported by clinical trial data to date, the potential significance of noninvasive brain stimulation is huge, affecting a large number of patients with debilitating conditions. Unfortunately, despite the rapid growth in interest and applications of these techniques, the physics and basic mechanisms of action remain incompletely explored, and biomedical engineering approaches that could lead to more effective stimulation devices, better suited for the specific applications, require careful consideration (for a more extensive history of noninvasive brain stimulation, please see the **Supplemental Appendix**, follow the Supplemental Material link from the Annual Reviews home page at **http://www.annualreviews.org**).

TMS: transcranial magnetic stimulation

tDCS: transcranial direct current stimulation

rTMS: repetitive transcranial magnetic stimulation

The two most commonly used techniques for noninvasive brain stimulation, transcranial magnetic stimulation (TMS) and transcranial direct current stimulation (tDCS), take advantage of different electromagnetic principles to noninvasively influence neural activity (**Figure 1**). TMS is a neurostimulation and neuromodulation application, whereas tDCS is a purely neuromodulatory intervention. TMS uses the principle of electromagnetic induction to focus induced currents in the brain. These currents can be of sufficient magnitude to depolarize neurons, and when these currents are applied repetitively [repetitive transcranial magnetic stimulation (rTMS)] they can modulate cortical excitability, decreasing or increasing it, depending on the parameters of stimulation, beyond the duration of the train of stimulation (1). During tDCS, low-amplitude direct currents are applied via scalp electrodes and penetrate the skull to enter the brain. Although the currents applied do not usually elicit action potentials, they modify the transmembrane neuronal potential and thus influence the level of excitability and modulate the firing rate of individual neurons in response to additional inputs. As with TMS, when tDCS is applied for a sufficient duration, cortical function can be altered beyond the stimulation period (2).

DEVICE DESIGN PRINCIPLES

Magnetic Stimulators

Magnetic stimulators consist of two main components (**Figure 2**): a capacitive high-voltage, high-current charge-discharge system and a magnetic stimulating coil that produces pulsed fields of 1–4 Tesla in strength with durations of approximately a millisecond for single-pulse stimulators and a quarter of a ms for rapid stimulators.

The charge-discharge system is composed of a charging unit, a bank of storage capacitors, switching circuitry, and control electronics. Without the switching circuitry and control electronics, the circuit is essentially a parallel RLC circuit, where the resistance, R, and the inductance, L, are both set to the lowest practical values to minimize heating while generating the desired waveform (mono-, bi-, and polyphasic devices exist, but the first two are most common). Single-pulse devices refer to those capable of delivering a stimulus every few seconds. Reverse charging or ringing in the circuit is prevented by placing a diode thyristor between the capacitor, C, and the inductor, L, thereby increasing the current decay time and eliminating reverse currents. In repetitive stimulators, the essential circuitry remains the same, except

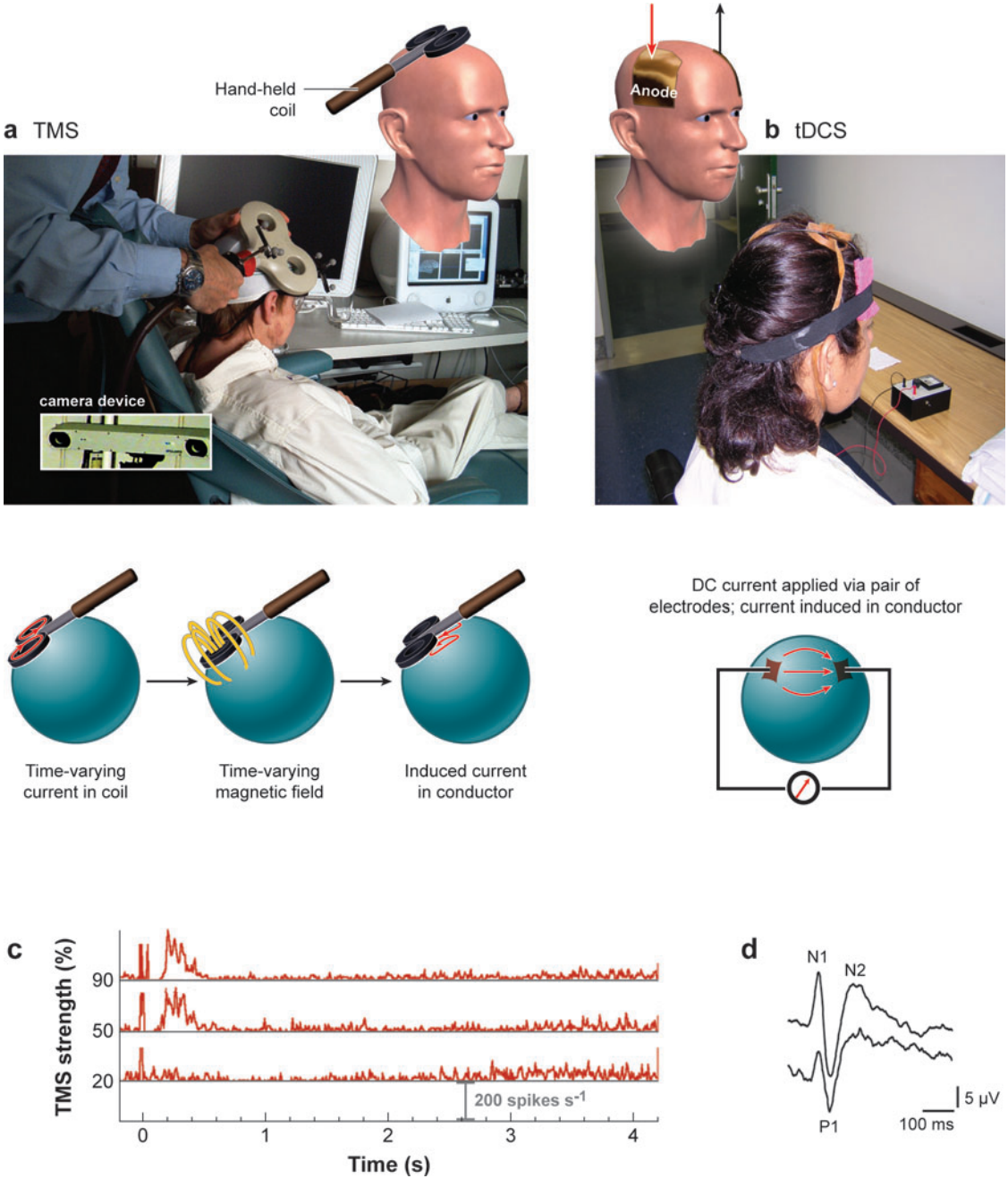

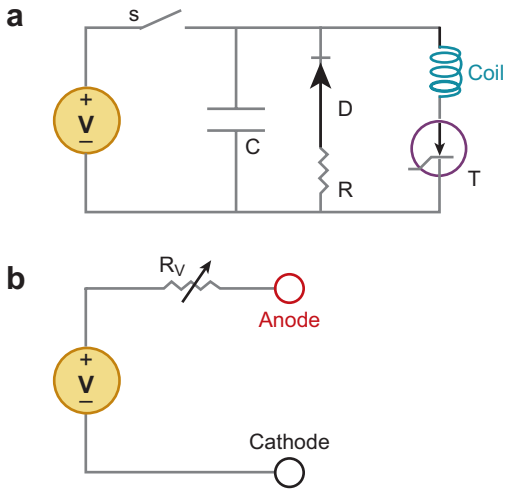

Figure 2

(*a*) A simplified circuit diagram of a single-pulse magnetic stimulator. (*b*) A circuit diagram of a tDCS stimulator unit. V = voltage source, s = switch, C = capacitator, D = diode, R = resistor, T = thyristor, R_V = variable resistor.

modifications are made to the switching system to allow pulse rates of many times per second (herein thyristor switching schemes can be used to recover energy to the capacitive charging unit and increase charging rates). Recent generation devices allow upward of 100 Hz stimulation frequencies. The difficulties in designing these machines relate to overcoming the high-voltage (400 V to more than 3 kV), high-current (4 kA to more than 10 kA), and high-power (where over 500 J of energy can be discharged in under 100 μs, or approximately 5 MW) demands on the circuitry while optimizing the device components to generate the appropriate coil current waveforms for neural stimulation. These topics are addressed in further detail elsewhere (e.g., 3).

The second key hardware component of magnetic stimulators is the current carrying coil, which serves as the electromagnetic source during stimulation. Design of the coil is critically important because it is the only component that comes in direct contact with the subject undergoing stimulation, and the coil's shape directly influences the induced current distribution and, thus, the site of stimulation (4, 5). Although many researchers have explored unique coil designs for increased focality (6–9) or specified stimulation (10–12), the most common coils currently used are

Figure 1

(*a*) During TMS, a time-pulsed current is discharged through a hand-held coil. The resulting time-varying magnetic field is focused onto underlying neural tissue. This field induces stimulating eddying currents in the tissue such that the neural activity can be affected during and after stimulation. The patient is shown wearing a device that can be used to predict the location of stimulation relative to the TMS coil, which is tracked via the camera device (*inset*); see text for more information about tracking systems. (*b*) During tDCS, a constant low-amplitude DC current is applied to the cortex via surface-mounted scalp electrodes. Neural activity can be affected during and after stimulation. (*c*) Effects as a function of TMS source strength. (*d*) TMS effects on event-related potentials.

single circular loop or figure-eight shaped (i.e., two circular coils in parallel, also referred to as double or butterfly coils; **Figure 1**). They are constructed from tightly wound copper wire, which are adequately insulated and housed in plastic covers along with feedback temperature sensors and safety switches. The choice of copper is primarily driven by its low electrical resistance, heat capacity, tensile strength, availability, and relative low cost. Exploration of other materials seems desirable as it might lead to means to construct smaller, and thus more focal, stimulation coils. Current limits are reached when the self-generated repulsive coil Lorentz forces overcome the tensile strength of the copper coils and cause them to shatter (5). Commercially available coil diameters range from 4 to 9 cm, with anywhere from 10 to 20 turns (typical coil inductances range from approximately 15μH to approximately 150 μH).

Some have explored the design of coils to attain subcortical stimulation (13, 14). Yet, it has been shown analytically that TMS currents will always be maximum at the cortical surface (15). However, it could be possible to develop a coil design where the rate of decay from the surface is attenuated, such that deeper structures can be stimulated (simultaneously with the overlaying cortical surface) without the need of excessive field strengths (13, 14). More recently, researchers have been investigating the use of conducting shields, placed between the TMS coil and the subject's head, to alter and focus the stimulating fields (16, 17). The use of nonlinear coil materials has also been explored, but has not been implemented commercially.

DC Stimulators

Currently, DC stimulation is applied via a constant current source attached via patch electrodes (surface areas from 25–35 cm^2) to the scalp surface (**Figure 1*b***). Currents usually range in magnitude from a constant 0.5 to 2 mA, and are applied from seconds to minutes. The electrodes can be simple saline-soaked cotton pads or specifically designed sponge patches covered with conductive gel. There is no complex circuitry comprising the stimulators, and in its simplest form a DC source is placed in series with the scalp electrodes and a potentiometer to adjust for constant current (**Figure 2*b***).

Tracking Systems: Localizing the Structures Targeted in the Subject's Brain

The current TMS standard for predicting the location of neural stimulation is based on image-guided frameless stereotaxic systems similar to those used for intracranial navigation during minimally invasive neurosurgery. No such system currently exists for tDCS; however, it is likely systems will be developed similar to those for TMS (with integrated field solvers), described below.

The frameless stereotaxic systems for TMS rely on the subject's head MRI data and coil geometry to digitally track the coil position relative to the subject's head and register the predicted stimulation location in MRI space (**Figure 1*a***). These systems work by first loading the subject's MRI data into the computer guidance system, then registering surface fiducial points of the subject's head within MRI space relative to a fixed optical or electromagnetic sensor on the subject's head, and finally tracking the

stimulating coil relative to the surface fiducials and a sensor affixed to the coil. Some systems exist that implement spherical model solutions to approximate current distributions in the cortex. Although these prediction methods are a major improvement on earlier methods, they ignore the electromagnetic interaction between the stimulating fields and the actual tissues that comprise the physical site of stimulation and provide no information as to the true stimulating current distribution induced within the subject's brain. It seems critically necessary to develop an integrated electromagnetic field solver tracking system to address these limitations, particularly given findings of current distributions in the setting of brain pathologies (see below).

PHYSICS AND FIELD MODEL FOUNDATIONS

TMS Foundations

During TMS, a time-pulsed magnetic field is focused on cortical tissue via a handheld coil to induce currents in the tissue. Phantom (4, 18–21), animal (22–24), and in vivo human studies (25) have provided important information on the induced current distributions. However, current technical limitations preclude the complete characterization of the electromagnetic field distributions via this type of experimentation and necessitate the development of theoretical modeling studies.

Numerous theoretical models have been developed to provide a view of the electromagnetic field distributions generated in biological tissue during TMS (26–36). Most models have been developed and solved with the finite element method, which is developed by segmenting the head tissues and defining tissue boundaries, assigning tissue conductivities and source parameters, and identifying current and voltage boundaries in the model region. The majority of earlier models were based on simplified shapes, such as infinite half-planes and perfect spheres. These models are typically solved for the electric field in terms of the time derivative of the magnetic vector potential owing to the coil current source and the secondary Laplacian field that results from the build up of charge at the conductive boundaries. Many of these earlier models are being reevaluated with the increased precision of more realistic head models, revealing important insights. For example, the simplified geometries of early models argued for the absence of currents normal to the cortical interface (20, 30, 37) and limited effects of surrounding tissues or altered anatomies (30, 32), but such conclusions have since been proven inaccurate by more realistic head models (33, 35, 38, 39). Results based on these simplified models have been misinterpreted in their application to clinical practice. For example, the conjecture that radial currents are absent during TMS has influenced the interpretation of clinical studies related to the generation of indirect (I) and direct (D) waves and justified the claim that interneurons tangential to the cortical surface are preferentially stimulated (40). However, such clinical interpretations need to be reevaluated in light of recent modeling work.

In 2002, Starzynski et al. implemented a more realistic head-shaped model consisting of a single homogeneous tissue, and they showed the importance of the head geometry in determining the final induced current density via a T-omega solution

FEM: finite element model

CAD: computer-aided design

method (41). In 2003, Nadeem et al. presented one of the most comprehensive models of TMS, demonstrating the importance of accounting for the actual head model geometry and tissue compartmentalization while calculating the induced current density magnitudes via the three-dimensional impedance method (36). The importance of the tissue properties were further highlighted by Miranda et al. who showed the effects of heterogeneities and anisotropies in a three-sphere mode in perturbing the TMS-induced stimulation currents (42). Wagner et al. generated a sinusoidal steady-state finite element model (FEM) based on an MRI-guided 3-D computer-aided design (CAD) rendering of the human head that included inhomogeneties, anisotropies, and additionally tested for the impact of alpha dispersion in tissues via a modified T-omega solution method (39). Although earlier TMS models only accounted for variations in tissue conductivities, alpha dispersion predicts that the actual low-frequency permittivity value of biological tissues could be high enough that displacement currents be relevant during TMS stimulation and the tissue permittivities can thus not be ignored (39). In this context, it is important to note, that during TMS, the main power components of typical current pulses are below 10 kHz (34), and classically the permittivity values implemented during TMS modeling generate quasi-static solutions with negligible displacement currents such that the permittivities can be disregarded. However, with the permittivity values predicted via alpha dispersion, the charge relaxation times of the tissue can be of the same order of magnitude as the timescale of the stimulating current source such that displacement currents need to be considered. Wagner's model was analyzed with permittivities spanning the magnitude range from 10^2–10^7 of the permittivity of free space for the various tissues, concluding that displacement currents are negligible up to permittivity magnitudes in the range of 10^5 of the permittivity of free space. Similar to other models, the maximum current density in the gray matter was found along the CSF/gray matter interface (**Figure 3*a*** displays the solution for when displacement currents were negligible). The ratio of maximum cortical current density to source strength ranged from (5.13×10^{-8} A/m^2 in the cortex)/(1 A/s source) in solutions with negligible displacement currents, to (5.51×10^{-7} A/m^2 in the cortex)/(1 A/s source) for the tissues modeled with permittivity values in the 10^7 magnitude range, a value of 2.9 A/m^2 to 31.1 A/m^2 for a 5 kHz 1800 A peak current source (5.65×10^7 A/s). Stair step jumps in the

Figure 3

(*a*) Plots of the current density magnitudes on the cortical surface for the TMS (*left*) and tDCS (*right*) solutions. The location of the stimulation source is depicted to the right of the current density magnitude solutions, both graphically over the 3-D models (*top*) and with the source shown above the solution (*bottom*). The coil (*gray*) represents the TMS solutions, whereas the anode (*red*) and the cathode (*black*) represent the tDCS solutions. (*b*) Current density magnitude evaluated along an evaluation line in the TMS and tDCS solutions. Note that the current density magnitude varies with the conductivity of the tissues. The insets show the mesh model with the current density magnitudes plotted on the surface of the cortex with the center evaluation lines shown intersecting the tissues. (*c*) Current density vector plots on the gray matter surface for the TMS and tDCS solutions. Note that the scales are normalized to the corresponding stimulation method, where the maximum for TMS is 2.9 A/m^2 and the maximum for tDCS is 0.103 A/m^2 at the anode. Modified from References 44, 57.

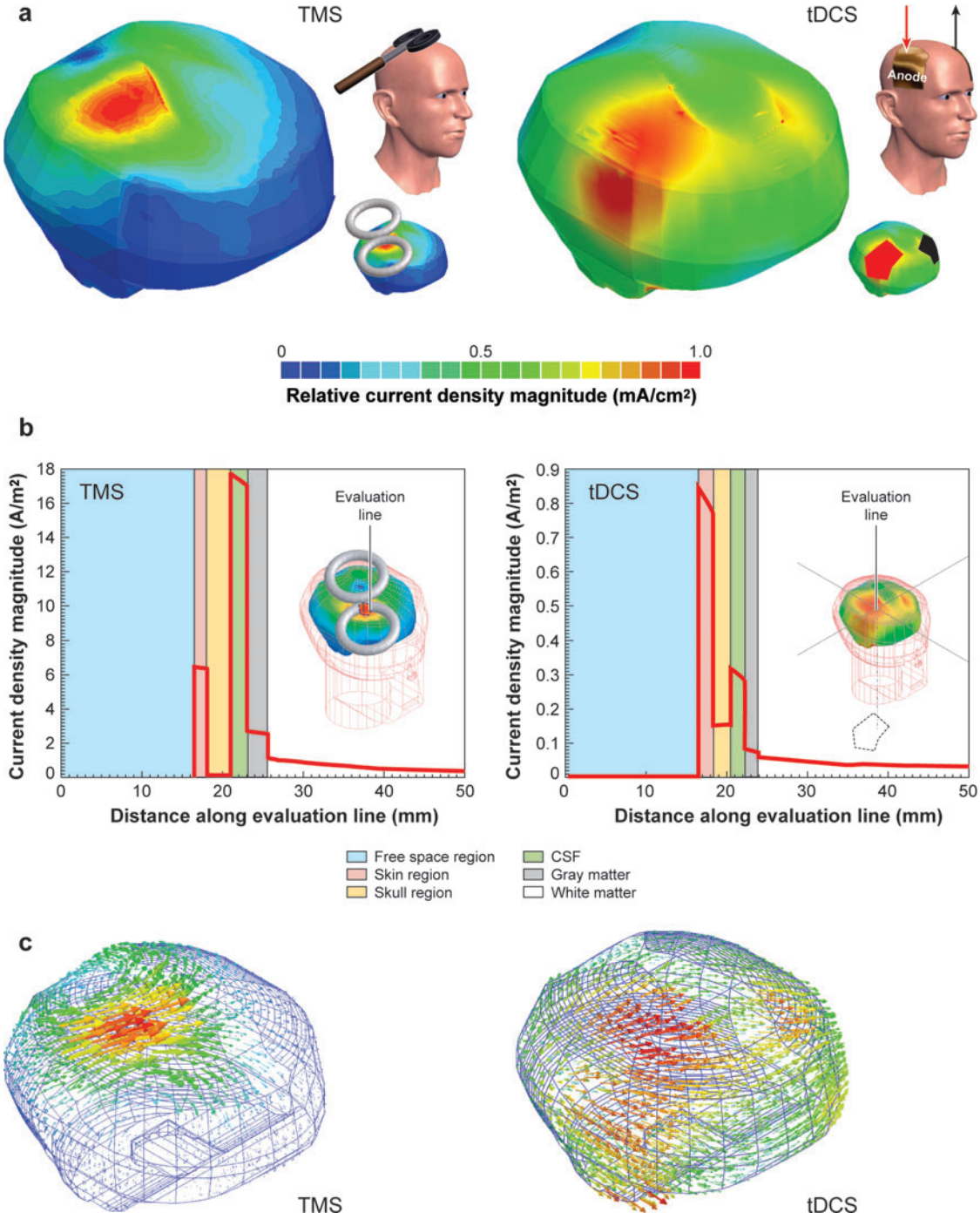

current density magnitude were seen at the tissue boundary interfaces in every solution and correlated with the magnitude of the complex conductivity of the tissue (complex conductivity $\sigma^* = \sigma + j\omega\varepsilon$) (**Figure 3*b***). The maximum cortical current surface area, defined as the surface area on the cortex where the current density was greater than 90% of its maximum, ranged from 107–119 mm^2 for the varied solutions, with slightly larger areas seen in the case of higher tissue permittivities. These surface areas are much larger than those predicted by simplified models, which claim functional stimulation areas as low as 5 mm^2. For all of the solutions, the location of the maximum cortical current density did not correspond directly to the location of the normal projection from the figure-eight-shaped coil's center, but this projection consistently intersected the cortex within the maximum cortical current surface area. The induced current density variation and vector behavior seen in the tissues were consistent with those of previous studies, where the vector orientation followed a figure-eight path with the greatest irregularity at the tissue boundaries (26, 37, 39) (**Figure 3*c***).

Future extensions of these methods could be used to develop a field solver coupled to a MRI frameless stereotaxic tracking system to predict the location of peak current density in the cortex and the relative current density distribution to neural orientations. Eventual combination of such a model with information gathered from diffusion spectrum imaging might prove particularly valuable in guiding optimization of induced current directions. In any case, it seems clear that there remains an unmet need for further in vivo tissue studies to ascertain the proper electromagnetic tissue properties to implement during TMS field model studies.

DC Stimulation

tDCS is a steady ohmic conduction process. To have a full understanding of the injected current distributions, one must either make direct measurements of the current distributions in either an animal or human subject under varied tDCS conditions with a sparse multipolar electrode grid or by constructing similar continuum electromagnetic models that take into account the true head anatomy, tissue properties, and electrode properties. Depth electrode recordings have been made to access the potential differences found during DC stimulation in three patients undergoing presurgical evaluation for epilepsy, finding potential values in the cortex ranging from 6.4 to 16.4 mV/cm for a 1.5 mA source (43), but more detailed experiments to more fully discriminate the field have yet to be made. Thus, herein we analyze multiple continuum models of electrical stimulation to more fully depict the injected current distributions.

A simplified resistor model provides an intuitive glimpse of the mechanism of DC stimulation (44), which predicts axial and tangential cortical current densities of 0.093 and 0.090 A/m^2 when approximating a constant area of stimulation (modeled with 7×5 cm electrodes in this case with 1 mA current strength). These current densities are of the same order of magnitude as those seen by Bindman to alter the level of neural excitability (45, 46). However, the true current distributions and the effects of the anatomical, tissue, and electrode variations need to be explored through

continuum electromagnetic models of the tDCS head system. Few electromagnetic models of tDCS presently exist, and thus numerous researchers rely on models of transcranial electrical stimulation (47–51), which do not completely account for the stimulating conditions used clinically or analyze the problem reciprocally based on early electroencephalography (EEG) models (48).

EEG: electroencephalography

TES: transcranial electrical stimulation

Transcranial electrical stimulation (TES) is similar in nature to tDCS in that an electrical source is used to stimulate cortical neurons; however, the electrodes applied, current sources used, and desired effect all differ. TES employs smaller electrodes than tDCS scalp electrodes, leading to much larger stimulating current densities (oftentimes applied as pulse trains, time-varying signals, or constant currents) compared to tDCS (applied as a time-invariant constant amplitude currents ramped on only at the onset of stimulation). Moreover, TES actively evokes action potentials from the underlying neural substrate, whereas the effects of tDCS alter the overall excitability of the neural response. The use of TES in awake humans is limited owing to the induced pain resulting from strong activation of skin and scalp pain receptors. TES is typically applied to evaluate active CNS functions during neurosurgery, whereas tDCS is used to modulate cortical activity following stimulation (2) (52). Although it differs significantly from tDCS, electromagnetic models of TES provide significant data about the current density distributions expected during tDCS. The quasi-static field approximation, which is implemented with both TES and tDCS electromagnetic models, implies conservation and linearity of the electric field solution such that different electric field and current density values can be linearly extrapolated from similar situations.

Multiple models of TES exist (47–51). Similar to tDCS, the frequencies of the stimulation source are such that they can be considered electroquasi-static (save for the possibility of alpha dispersion effects discussed above) in nature and evaluated in terms of the electric potential (φ), by solving Laplace's equation,

$$\nabla \cdot (\sigma_i \nabla \phi) = 0, \tag{1}$$

where σ_i is the conductivity of the tissue. A number of common results relevant to tDCS stimulation have been demonstrated: (*a*) the skull's high resistivity attenuates the currents reaching the cortex, which instead are primarily shunted along the scalp surface; (*b*) the geometry of the head and the tissue electromagnetic properties play a significant role in determining the final field distribution; and (*c*) the electrode placement is critical to determining the final field distribution.

Wagner et al. have produced a new FEM specific to tDCS (**Figure 3**), which tested various electrode montages used in clinical investigations and analyzed the role that tissue heterogeneities and anatomical variations play on the final current density distributions (44). For all of the solutions, similar trends, captured in TES modeling and enumerated above, were seen. The current density magnitudes varied substantially throughout the tissues and stair step jumps in the current density occurred at each tissue boundary reflective of the varied tissue conductivities (**Figure 3*b***). While varying the electrode placement and keeping a constant current source (1 mA/35 cm^2 surface electrode area), the maximum local cortical current densities ranged from 0.077 to 0.20 A/m^2 (note that separate maximums were found on the cortical surface

in the region of both the cathode and the anode, but obviously of reversed polarity), whereas scalp current densities ranged from 8.85 to 17.25 times larger in magnitude than the cortical current densities (**Figure 3*a***). While varying the electrode area (from 1–49 cm^2 with a 1 mA constant current) and keeping the placement fixed (anode over the right M1 and cathode over the left supraorbital), the maximum cortical current densities ranged from 0.081 to 0.141 A/m^2 in a nonlinear fashion, reflective of the relative anatomical/geometrical effects on stimulation current densities (**Figure 3*c***). The shunting (i.e., the flow of current along the scalp surface as opposed to the cortex) effects were considerably larger for the 1 cm^2 electrodes compared to the other montages, where current densities in the skin were as much as 86 times greater than those seen in the cortex for the 1 cm^2 electrodes compared to a factor of 8.56 for the 49 cm^2 electrodes. Essentially, greater shunting occurs with smaller electrode areas, indicative of the varied resistive paths. This is important when one analyzes the results of earlier tDCS studies that implemented varied electrode types, of varied geometries, often with mixed results, quite possibly owing to this shunting effect. Although the cortical current density magnitudes are far lower than action potential thresholds from controlled electrical stimulation experiments of cortical neurons [0.079 to 0.20 A/m^2 compared to 22 to 275 A/m^2 (53)], these tDCS magnitudes have been shown to influence spontaneous activity and characteristics of the evoked response from cortical neurons (45, 46, 54). This suggests that the mechanisms of action of tDCS may be quite different from that of TMS, TES, direct cortical stimulation, or even deep brain stimulation, even if behavioral effects may appear similar.

Modeling in the Presence of Pathologies

With TMS, changes in the tissue anatomy and electromagnetic properties have been shown to alter the TMS-induced stimulating currents in both phantom and modeling studies (39, 42, 55, 56). As such, continuum field models provide researchers with a means to explore the effects of pathological alterations in the cortex on the TMS-induced and tDCS-injected stimulating current densities. Wagner et al. (57) compared the TMS field distributions in the healthy head models with those resulting from electrical tissue property and anatomical alterations caused by stroke (**Figure 4**), and similar comparisons were made for other pathologies (e.g., atrophy, tumor) and tDCS current densities (44). For each of the pathologies, the TMS-induced and tDCS-injected currents were significantly altered for stimulation proximal to the pathological tissue alterations for all of the models analyzed. The current density distributions were modified in magnitude, location, and orientation such that the population of neural elements that was stimulated was correspondingly altered. The main reason for this perturbation is that the altered distribution of brain tissue modifies the conductivities in the pathological regions and effectively provides paths of altered resistance along which the stimulating currents flow. These cortical current density perturbations could prove to be dangerous or, at the very least, lead to unreliable, erroneous results if guided by models that do not account for the electromagnetic tissue interactions.

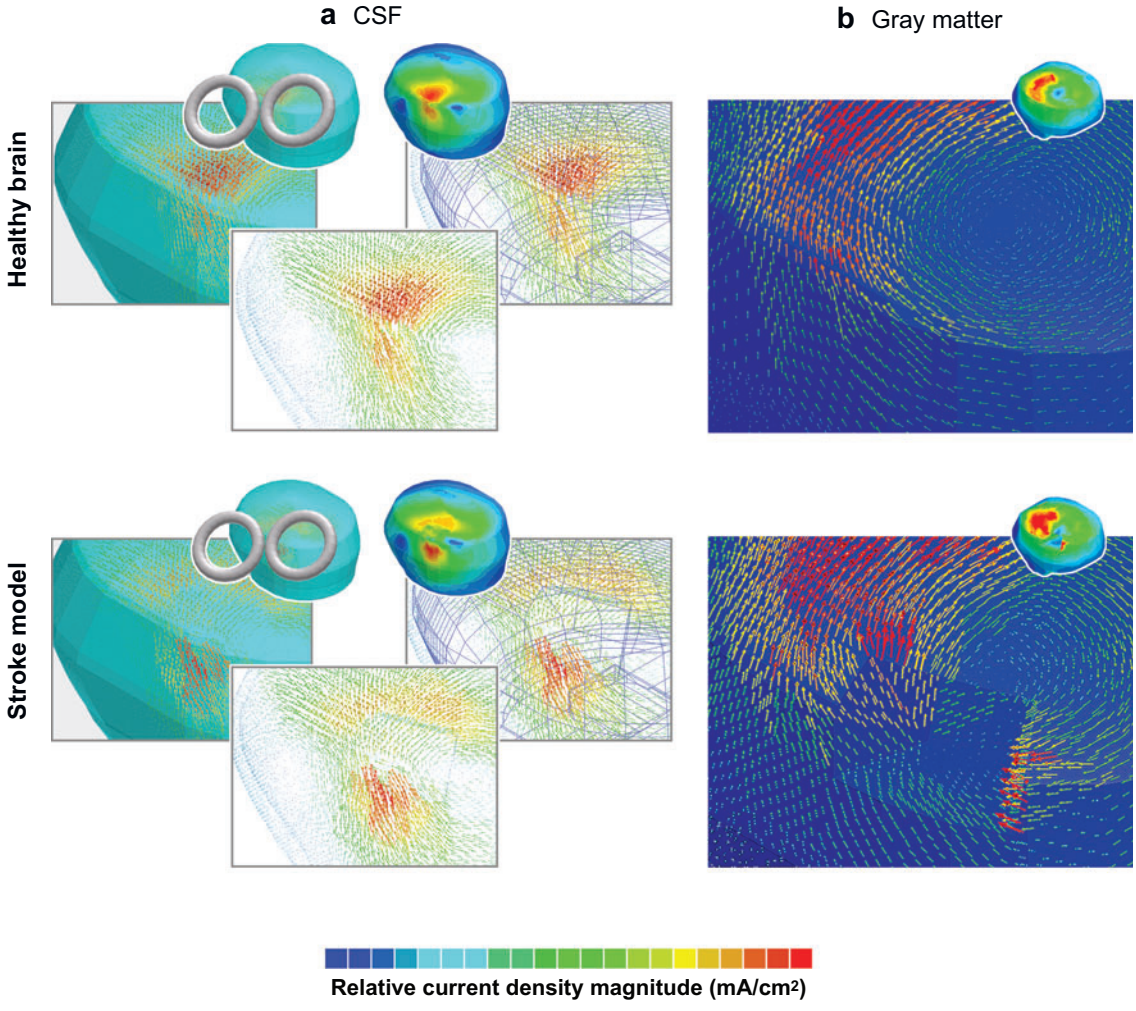

Figure 4

(*a*) Current density vector distribution in the CSF, comparing a healthy head model and a stroke model. Note that in the CSF, the current is directed from its predictable course in the healthy head model toward the underlying stroke borders. (*b*) Current density vector distribution displayed on the cortical surface for healthy head versus stroke models. In the stroke model, the current density vector distributions deviate from predictable figure-eight distributions that are seen in the healthy head model to conform to the infarction boundaries. The current vectors became more perpendicular to the stroke boundary along its border and particularly focused at the corners where the areas of maximum cortical current density were found. Modified from References 44, 57.

ELECTROPHYSIOLOGY OF STIMULATION

Although so much is still unknown about the electromagnetics of TMS and tDCs, even less is known about the neural mechanics of activation. Most models of neural stimulation are mathematical extensions of the Hodgkin & Huxley model. Of these, the one that is most accepted and cited for TMS is the Roth peripheral nerve model, a modified active-cable-type model (29, 30, 58–60). This model is similar to peripheral nerve models of electrical stimulation (61–63).

The passive cable model that is the foundation for the Roth model is based on classic transmission line theory, where the transmembrane potential, V, can be represented by the following equation:

$$\lambda^2 \frac{\partial^2 V}{\partial x^2} - V = \tau \frac{\partial V}{\partial t}, \tag{2}$$

where $\lambda = \sqrt{\frac{r_m}{r_i}}$, $\tau = c_m r_m$, r_m is the membrane resistance times a unit length, c_m is a membrane capacitance per unit length, and r_i is the axoplasm resistance per unit length.

The passive cable model (Equation 2) can be altered by adding an activating function to represent an external current source, as seen during electrical stimulation, or by adding the induced electric field, as seen during TMS. Here, the equation is altered to include a TMS source:

$$\lambda^2 \frac{\partial^2 V}{\partial x^2} - V = \tau \frac{\partial V}{\partial t} + \lambda^2 \frac{\partial^2 \mathrm{A}}{\partial x \partial t}, \tag{3}$$

where $-\frac{\partial \mathrm{A}}{\partial t}$ represents the induced electric field. This is similar to electrical stimulation models that include activating functions (62). This model predicts conduction along the membrane when the activating function is below the neural threshold.

To further increase the detail of the model, one could include the active properties of the axon by implementing the Hodgkin & Huxley model (64), which includes the voltage/time-dependent sodium and potassium channels represented by g_K and g_{Na} (conductances per unit area for sodium and potassium), respectively; the static leakage channel represented by g_L; and the Nernst potential for the sodium, potassium, and leakage ions represented by E_{Na}, E_K, and E_L, respectively. With these additions, the final equation of Roth's model is

$$\lambda^2 \frac{\partial^2 V}{\partial x^2} - g_L(E_L - V) - g_{\mathrm{Na}}(E_{\mathrm{Na}} - V) - g_k(V - E_K) = C_m \frac{\partial V}{\partial t} + \lambda^2 \frac{\partial^2 \mathrm{A}}{\partial x \partial t}, \tag{4}$$

where $\lambda = \sqrt{\frac{1}{2\pi a^2 r_i}}$, a is the axon radius, and C_m is given as capacitance per unit area. Much work in the field of electrical stimulation has been done by Rattay (62) and others based on similar theoretical models.

According to Roth's model, the site of neural stimulation (the initiation of action potentials) is found where the spatial derivative of the induced electric field is maximum. One consequence is that the coil hot spot of a figure-eight coil does not correspond to the optimal site of peripheral nerve stimulation. Predictions based on this model have been assessed experimentally—clearly agreeing in some studies (65) but not in others (66). Finally, it should be clear that this model pertains only to long peripheral nerves and there is no justification to extend this model to cortical

neurons. In fact, if the same field parameters used for this model were used for cortical neurons, the spatial gradients of the electric field would be negligible due to the cortical neurons' short length except at locations of axonal bends.

Another model that more accurately depicts cortical neurons is the cable model developed by Nagarajan (67–70), which, by incorporating boundary-type equations, begins to account for the smaller size, branching, and terminal endings found in cortical neurons. With this model there are two activation functions, one owing to the boundary fields and one owing to the induced electric field gradient along the neural fiber axis. With this increased complexity, the spatial derivative of the induced electric field is not the primary factor in predicting the activation site as it was in the Roth model; instead, the field effects at the boundary dominate. In the Nagarajan cable model, the excitation site is located at the axon terminals (bouton locations) or at the cell body, where the neural axon begins. According to the model for "short axons with sealed ends, excitation is governed by the boundary field driving function which is proportional to the electric field" (70). In the field of electrical stimulation, similar models have been produced that render similar results (dependent on the stimulus waveform) (63), but have not yet fully explored the effects of DC currents.

There have been few attempts to explain the biophysical mechanisms of TMS stimulation and we are unaware of any relevant biophysical models of altered membrane excitability owing to weak DC currents in TMS. However, Kamitani et al. (71) generated a model to offer insight into the physiology of TMS stimulation. With a realistic cell model that took into account the dendritic aborization, synaptic inputs, and the various densities of the sodium, potassium (slow and fast channels), and calcium channels, they were able to show a few key results, most notably, that the induced current within the neurons was directly related to the electric field along the neuron path. Without a synaptic background, magnetic stimulation rarely reached threshold, whereas with a background of synaptic inputs, magnetic stimulation brought about burst firing followed by an extended silent period. Bursting was brought about by an influx of Ca^{2+} ions followed by the opening of Ca^{2+}-dependent K^+ channels, which would then limit the effects. Such a result could be the cause for the post-stimulatory effects of TMS via long-term potentiation mechanisms.

With both tDCS and TMS, electrophysiological studies have been completed to explore the effects of the electromagnetic fields on the cortices and the neural elements. In 1956, Terzuolo et al. studied the effects of DC currents on neural preparations and the relative orientations of current to the axon. They found that currents as low as 3.6×10^{-8} injected across the preparation region could change the frequency of firing, even though they did not directly initiate an action potential (72). In the 1960s, Bindman showed that currents as low as 0.25 $\mu A/mm^2$ applied to the exposed pia by surface electrodes (3 μA from 12 mm^2 saline cup on exposed pia surface) could influence spontaneous activity and the evoked response of neurons for hours after just minutes of stimulation in rat preparations (45, 46, 73). Purpura et al. (54) showed similar effects in cat preparations for currents as low as 20 $\mu A/mm^2$ from cortical surface wick electrodes ranging in area from 10–20 mm^2. In 1986, Ueno et al. completed work with neural preparations and time-changing magnetic fields to ascertain their effects on action potentials. However, constraints with the experimental design

originating from a resistor that was impaled into the neural preparation throughout the experiments (74) limit the impact of this work. Maccabee et al. (75) studied the use of peripheral nerve preparations to represent cortical fiber bends (bent fiber model) and found "excitation at the terminations takes place at much lower thresholds and it occurs at a site within the peak electric field," similar to the cable models of Nagarajan (70). McCarthy & Hardeem (76) conducted a number of experiments with neural preparations and pulsed toroids, and they came to the controversial conclusion that capacitive, not inductive, effects were the cause of magnetic stimulation. Although, they implemented sources outside of the power spectrum of typical stimulators, their results are interesting when considering dispersion-dependent Hodgkin and Huxely models (76a).

In terms of the network activity, little is known regarding the biological effects of TMS or tDCS. Currently, only one single network model of TMS (77) exists, accounting for more than 33000 neurons with approximately 5 million modeled synaptic connections, which clearly reproduces many experimental TMS results. Although Esser's model begins to explore network dynamic effects of TMS, future expansions of the model will clearly bring insight into the network dynamics of stimulation and the future therapeutic applications of TMS. As discussed below, 2-DG imaging studies of rTMS in animals have clearly demonstrated that network effects are not physiologically confined to one brain site (78). However, no quantitative model has been developed that clearly explains the role that rTMS plays in altering cortical, and thus network, excitability. The network effects of tDCs have been similarly underexplored.

Regrettably, there is no clear understanding of the true biophysical dynamics of TMS or tDCS. With TMS, the models that exist bring up many relevant issues, but unfortunately they have not been tested on a cellular level owing to the technical difficulties associated with the process. Until a methodology that will not be corrupted by the field artifact is implemented, analogies between microstimulation and TMS will be the primary approach on which researchers have to rely. With tDCS, little work has been done to ascertain the cellular effects of the weak currents. The technological hurdles that exist with TMS are not present with tDCS. Hopefully, future work will shed more light on both processes.

INSIGHTS FROM ANIMAL EXPERIMENTS

One of the most surprising aspects of noninvasive brain stimulation methods such as TMS and tDCS is that their scientific and clinical applications have largely preceded—instead of followed—an extensive development of animal models aimed at determining the details of their neurobiological effects. This could be understandable given their lack of invasiveness and apparent short duration of their effects in the intact human brain. However, as a result, the understanding of the detailed spatial and temporal dynamics of specific patterns of stimulation and their detailed neurobiological effects remains insufficient. Given the progressive mainstream spread of TMS- and tDCS-based therapeutic approaches, the use of adequate animal models to preassess the effectiveness and long-term safety of increasingly aggressive therapies becomes a real need. A useful animal model needs to allow for the combination

of a precise and reliable stimulation method with monitoring tools of high spatial and temporal resolution to capture the physiologic impact. Monitoring methods of high spatial resolution include metabolic/pharmacologic labeling, optical imaging, and high-field functional magnetic resonance imaging (fMRI). Monitoring methods of high temporal resolution are field- or single-unit electrophysiological recordings. Ideally, both of these types of monitoring methods should be combined and applied simultaneously. Furthermore, an ideal animal model should allow for the exploration of the behavioral correlates of the stimulation in the awake, freely moving animal. A pre-existing knowledge on the anatomical connectivity between regions and the effects of other types of brain manipulation in the same regions, such as lesion studies, pharmacologic deactivations, microstimulation, or cooling deactivations, is obviously enormously helpful in the interpretation of the results, helping to rule out potential epiphenomena.

fMRI: functional magnetic resonance imaging

Rodents (79–86), felines (78, 87–91), and in a very limited fashion nonhuman primates (92) have been used in TMS studies aimed at understanding the physiology underlying its effects. Excluding some of the pioneer reports (46, 54), recent equivalent studies using tDCS remain scarce and are limited to testing its therapeutic effects in rodent models of migraine and epilepsy (93, 94). Especially for TMS, the ratio between head size and coil size remains the main issue precluding an easy interpretation and transferability of animal results into human applications because the induced current density distribution and the spatial selectivity of the impact are strongly affected by the thickness and size of the brain (95). This is particularly critical for rodent models, in which spatially selective repetitive stimulation of specific neural networks will remain unfeasible, unless smaller TMS coils can be designed (85, 86, 96). The limited number of nonhuman primate TMS experiments can be explained by its high cost, the difficulties in training such species to calmly tolerate periods of stimulation, and the continuous twitching induced by TMS pulses in their powerful jaw muscles, thus it needs further development. By using an acceptable coil size/brain size ratio, the cat model has provided the most valuable body of data on the underpinnings of TMS impact.

In the anesthetized animal, Funke et al. reported the first direct evidence on how TMS single or double pulses "interfere" with the firing of specific visual neurons tuned to the processing of a given orientation, eliciting different episodes of enhanced (<500 ms post TMS pulse) and suppressed activity (from 500 s to a few seconds) (87, 88). Those patterns proved to be pulse-intensity dependent, so that higher stimulation generated an additional early suppression wave of 100–200 ms duration. In spite of their temporal accuracy, such localized single-unit recordings are "blind" to the contribution of local and distant re-entry mechanisms, which might operate such complex and long-lasting suppression-activation dynamics, resulting in lasting neuromodulation. Using a different approach, Valero-Cabre et al. (78) combined rTMS stimulation in extrastriate parietal regions involved in spatial processing, with 2-deoxyglucose uptake labeling of the whole brain volume. Taking advantage of their high spatial resolution (100 μm), those studies provided direct evidence of the network effects of cortical rTMS on an extended network of cortical, subcortical, and midbrain nodes linked by specific anatomical pathways (**Figure 5**). High-frequency

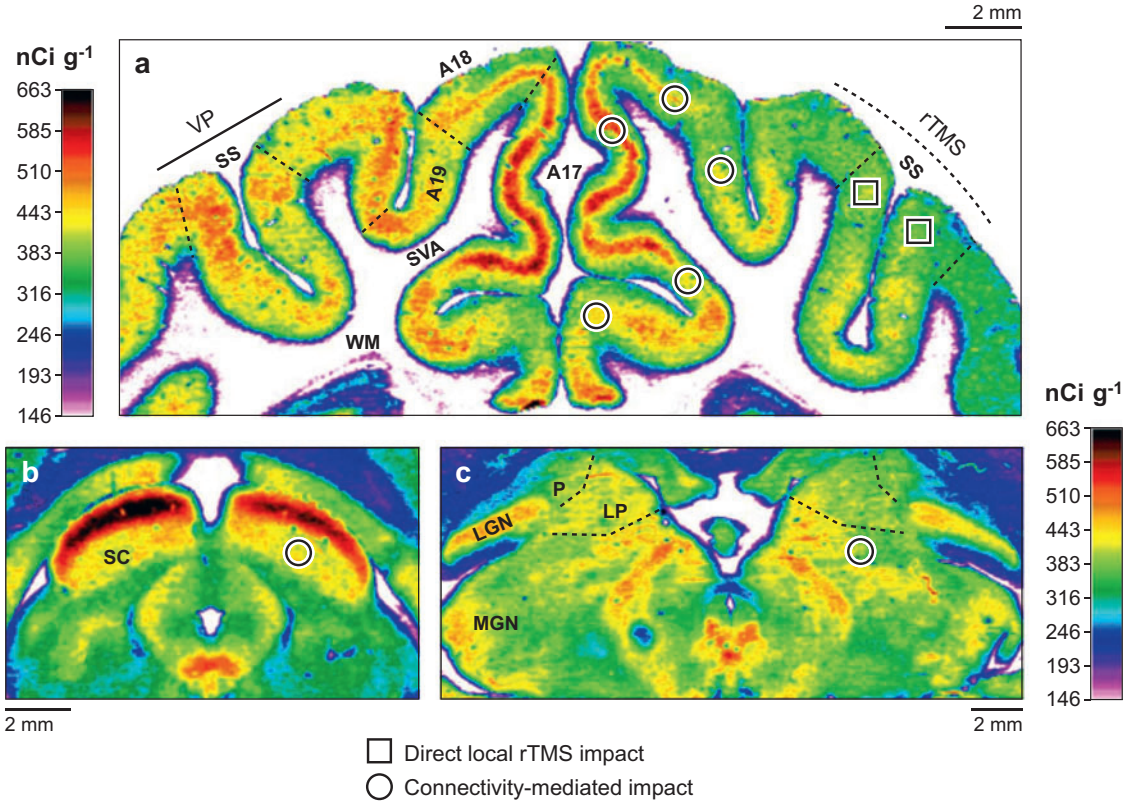

Figure 5

Local and network effects of "on-line" rTMS on neural systems in cats. (*a*) ^{14}C-2 deoxyglucose (2DG) uptake image from a cat brain submitted to 20 Hz rTMS on the left visuo-parietal (VP) cortex which is located at both sides of the suprasylvian sulcus (SS). This region is homolog to human posterior parietal regions and is involved in spatial processing. Note the differences between the stimulated and the nonstimulated regions in the contralateral hemisphere. Regions of the VP are directly targeted by rTMS stimulation (*squares*). Other regions—SVA, CVA, A18, A19 and A17—are transynaptically deactivated by the reduction of the excitatory drive exerted from the VP cortical areas targeted with rTMS (*circles*). VP = visuo-parietal cortex; SS = suprasylvian sulcus; A17, A18 and A19 = primary visual areas 17, 18 and 19; SVA = splenial visual area; CVA = cingulate visual area; WM = white matter tracts. (*b*) Detail of connectivity-mediated rTMS transynaptic deactivation on the superficial layers of the superior colliculus (SC) of the same side of the targeted VP cortex. (*c*) Levels of ^{14}C-2DG activity in the posterior thalamic nuclei (such as P and LP) of subjects that received unilateral rTMS onto the VP cortex of the same side. Regions holding no connectivity with the VP cortical region do not reveal any significant difference in glucose metabolic activity. Levels of 2-DG uptake are measured in nCi g^{-1} of tissue, represented by the color spectrums next to each image. P = pulvinar, LP = lateral posterior complex, LGN = lateral geniculate nucleus, MGN = medial geniculate nucleus. Modified from Reference 78.

stimulation generated a mean 14% decrease in cortical activity, affecting a radial area of ~12 mm^2 (**Figure 6*a***) and a ~1.25% attenuation effect per each mm of cortical depth across a sulcus separating two banks of cortex (**Figure 6*b***).

Further findings demonstrated that local and transynaptic effects of TMS depend on stimulation frequency and time of the assessment in a rather complex way. During the delivery of the TMS pulses ("on line impact"), cortical activity is strongly locally depressed, inducing prominent transynaptic effects. This is likely to be the result of significant pools of the targeted cortical neurons being repetitively depolarized, thus interfering with their normal encoding firing rhythms. Opposite modulation in cortical metabolism dependent on stimulation frequency patterns were found, outlasting the delivery of TMS trains ("off-line" impact or "after effects") (90). High- or low-frequency patterns of stimulation resulted in significant increases and decreases, respectively, of local glucose consumption, thus providing support to uses of rTMS in neuromodulation of brain systems (**Figure 7**). These results are in agreement with similar and recent cat studies using EEG and evoked visual potentials (91). This frequency-dependent effect seems to suggest LTP-, LTD-like modulation of the targeted systems (80, 97, 98) and might also reflect the contribution of compensatory mechanisms emerging from "untouched" brain networks (99). The majority of such invasive studies are mainly performed in the anesthetized animal, ruling out behavioral and nonspecific TMS side-effects. Congruent behavioral and metabolic correlates of similar stimulation patterns are being explored in awake intact and brain-injured cats.

Transcranial DC stimulation has proven to induce both immediate and long-lasting changes through a completely different set of mechanisms. According to early studies in rodents, tDCS generates single-unit firing enhancements during surface anodal stimulation and decreases during cathodal stimulation (46, 54). These effects are thought to be mediated by changes in the resting membrane potential of the stimulated region, but the spatial resolution of the effects and its potential network impact remains to be studied in detail in larger animals using analogue neuroimaging and electrophysiological methods, as those reported for TMS.

Animal models will be instrumental to further understand the impact of noninvasive brain stimulation techniques, to optimize scientific and clinical applications of these techniques, and to test emerging technologies and ensure their safety. Thus, future endeavors need to explore the use of awake performing animals, such as cats or possibly nonhuman primates, and combine whole-brain, high-resolution imaging techniques, such as fMRI, with multielectrode field and/or single-unit recordings.

MERGING TMS WITH OTHER BRAIN-IMAGING METHODS IN HUMANS

Merging TMS with other brain-imaging techniques provides particularly powerful means to explore brain function in the living human brain, understand brain-behavior relations, and optimize the impact of brain stimulation techniques. Insights from such experimental approaches can meaningfully be contrasted with results from animal experiments and guide further sophistication and testing of modeling approaches. Electroencephalography (EEG) and evoked potentials offer exquisite temporal

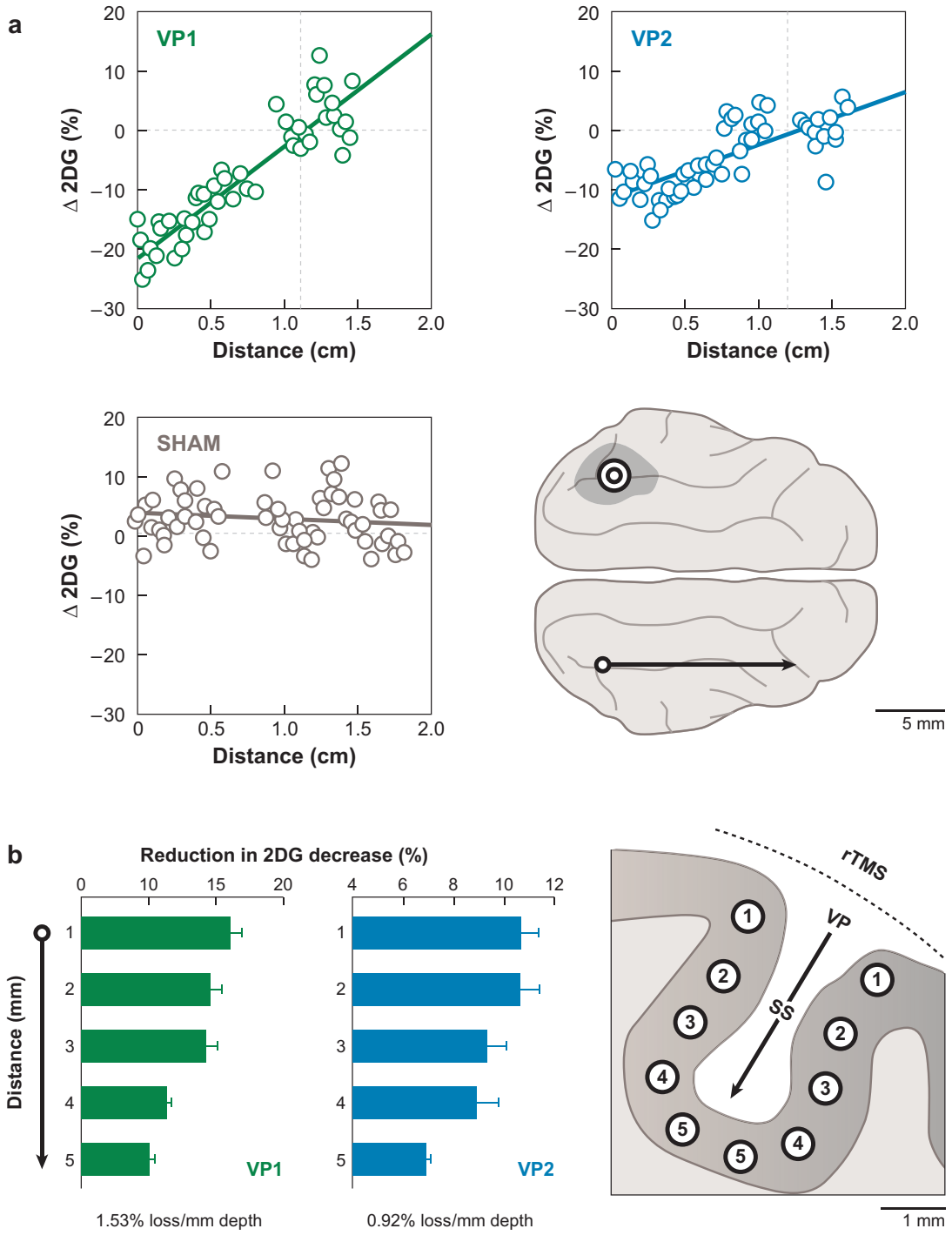

resolution and direct measures of neuronal activity. fMRI delivers maximal spatial resolution. Positron emission tomography (PET) can be used to measure glucose or neurotransmitter receptor uptake to gain insights into the metabolic impact of brain stimulation. Optical brain imaging, single-positron emission tomography, diffusion tensor imaging (DTI), and other brain imaging modalities also offer unique advantages. As proposed by Paus (100), it is possible to combine TMS or tDCS with various other brain imaging methods before, during, or after the stimulation.

PET: positron emission tomography

DTI: diffusion tensor imaging

Brain imaging before noninvasive brain stimulation techniques has as its principal objective the improved planning and precise guiding of the stimulation. MRI can be used in combination with stereotactic systems to define and monitor the site of stimulation. Functional information derived, for example, from fMRI, SPECT, or PET can be overlaid onto anatomical MRI information and be used to define the target of noninvasive stimulation techniques. In this context, it is important to remember the possible limitations of projections of the main stimulation vector and the desirable benefit of more realistic models of induced currents in the human brain, particularly in the setting of brain pathologies (see above). Nonetheless, using such approaches, it is possible to use noninvasive brain stimulation to add causal information to the otherwise purely correlational insights of functional brain imaging. Furthermore, the use of EEG or evoked potentials can provide valuable temporal information as to when to deliver a stimulation pulse to maximize a desired behavioral impact.

The use of brain imaging after noninvasive brain stimulation (TMS or tDCS) is primarily aimed at revealing the changes in brain activity induced by the stimulation. Obviously, the stimulation will induce behavioral changes and thus the demonstrated changes in brain imaging will be a complex interplay of the correlates of the stimulation itself, the neurophysiologic consequences of the behavioral changes, and the response of the brain to such behavioral changes. Careful experimental designs are thus critical to isolate the desired measures. These challenges are further compounded by the fact that the combination of any brain-imaging method with TMS or tDCS is technically challenging and poses unique engineering difficulties owing to the risk of artifact. Such artifacts can obscure the brain imaging measures immediately after the brain stimulation and become a lot more troublesome for studies of brain imaging during TMS or tDCS.

Figure 6

(*a*) Correlation plots showing the individual percent change (Δ) between stimulated and unstimulated VP cortex, beginning at 0.0 cm in the posterior end of the suprasylvian sulcus (SS) to a distance 2.0 cm forward in the brain. The arrow shows the direction of data sampling in the VP cortex, presented in the correlation plots. We present data from two cats stimulated with real rTMS on VP (VP1, VP2), and a control animal (SHAM) stimulated with sham rTMS at the same region. The concentric circles (◎) indicate the exact site of TMS stimulation in the visuoparietal cortex (*shaded region*). Modified from Reference 78. (*b*) Notice the decay in the rTMS induced reduction of cortical metabolism generated on VP cortex. No significant changes in 2DG uptake were detected during sham rTMS stimulation. Regression functions for both animals allowed us to estimate the spatial resolution of our stimulation, i.e., the distance to complete loss of rTMS significant effect in the order of 10–15 mm. Modified from Reference 78.

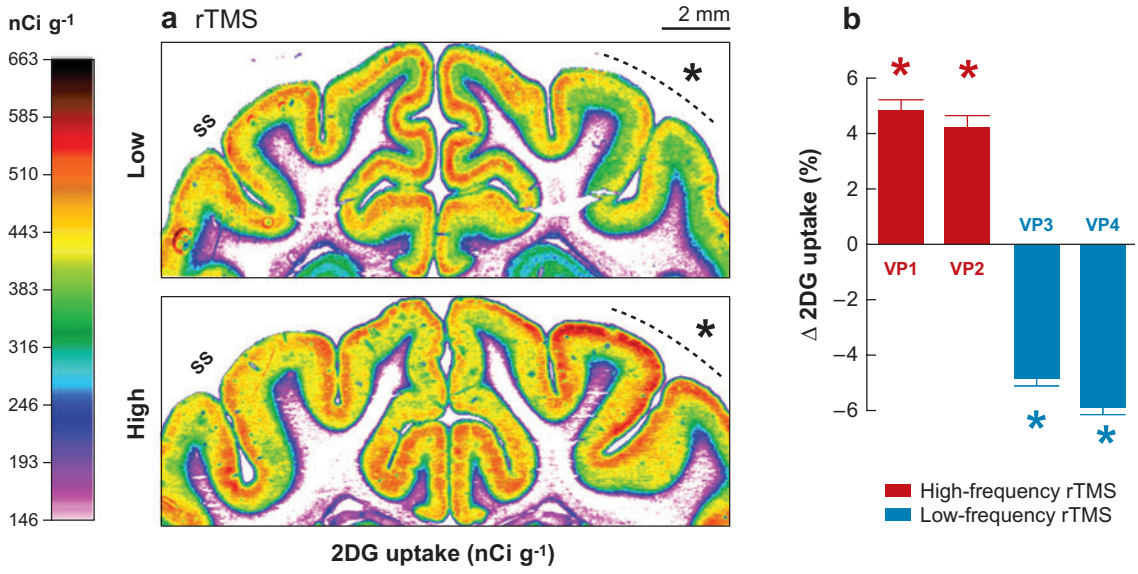

Figure 7

(*a*) Representative color-coded ^{14}[C]-2-deoxyglucose (2DG) uptake images and average histograms from a pool of four adult cats (subjects VP1-VP4) that received either high- (VP1, VP2) or low-frequency (VP3, VP4) rTMS stimulation patterns on the visuo-parietal (VP) cortex. Notice the intense long-lasting decrease of 2DG at the stimulated VP (*) in respect to its contralateral counterpart after ~20 min of high-frequency rTMS. Also note the decrease induced after the same period of continuous stimulation at low frequency. The impact of both interventions is much milder than that generated by "on-line" high-frequency stimulation, as shown in **Figure 5**, which is represented in an identical 2DG level scale. The asterisks (*) indicate the position of the rTMS coil located on the scalp right above the so-called suprasylvian sulcus (SS). (*b*) Histogram displaying the average percent change (Δ) in 2DG uptake after the application of high (*red*) or low (*blue*) frequency trains at parietal regions of four cats. Changes in local metabolic activity affected primarily the superficial regions of the crown of the SS. The deeper the region, the lower the change in activity that is produced. Detailed analysis demonstrates that the region of significant "off-line" rTMS impact extended ~1.5 to 1.8 mm^2 around VP. These data indicate that high-frequency stimulation induces extended increases of activity. On the contrary, low-frequency rTMS results in long-lasting metabolic decreases across the same region. Additionally, white matter or subcortical or distant effects were only rarely noted, thus indicating the long-lasting rTMS impact is mainly locally restricted to the targeted VP region. For both paradigms, sham TMS stimulation resulted in no changes in cortical 2DG uptake. Modified from Reference 48.

TMS and EEG

EEG was the first technique to be explored in combination with TMS (101). EEG provides exquisite temporal resolution and a direct measure of neuronal activity, and it is capable of differentiating between inhibitory and facilitatory effects. Initial studies combined EEG and TMS to study functional alterations at regions distant (in time and space) to magnetic stimulation via an analysis of altered EEG patterns. For example, it was possible to provide in vivo measures of transcallosal and fronto-parietal

interactions (102, 103). However, the value of the results was limited by the quality of the EEG signal, excessively distorted by artifacts related to the TMS pulses. Problems related to the saturation of the EEG-recording amplifiers from the TMS pulse have been overcome by artifact subtraction and pin-and-hold circuits, and by altering the slew rate of the preamplifiers. Thanks to these developments, it is now possible to analyze the EEG online with TMS stimulation (104, 105). This allows for the analysis of the effects of TMS on task-related electrophysiological recordings and provides information on various functional aspects of the large-scale networks involved in cognition, including feed-forward and feed-back mechanisms of functional signal transmission. It is clear that TMS-induced neuronal activity spreads beyond the directly stimulated area to anatomically connected sites and thus TMS ultimately induces a modulation of a specific, cortico-subcortical, bihemispheric neural network. Behavioral effects of TMS over a given brain area reflect how the distributed neural network (and the rest of the brain) reacts and compensates for the transient cortical disruption during task execution. The behavioral effects of TMS critically depend on anatomical and functional connectivity of the stimulated area, on the excitatory and inhibitory interplay between target area and connected sites while subjects carry out a given task, on the orchestration of serial and parallel processes across the regions operating in concert for task execution, and on the possibility to tap into functions whose neural bases were left unaffected by TMS. Therefore, precise control of the behavioral effects of TMS in a given individual requires (*a*) precise and consistent targeting of a defined brain region and (*b*) timing the stimulation and setting the stimulation parameters so as to guide activity in the targeted brain region and its connected neural network in a predictable and desired fashion. Timing the stimulation and setting its parameters so as to induce a defined modulation of activity in a distributed neural network requires online monitoring of the brain activity. Combined EEG-TMS techniques provide neuroscientists with a unique method to test hypotheses on functional connectivity, as well as on mechanisms of functional orchestration, reorganization, and plasticity. Combination of TMS with EEG can also serve to increase the safety of brain stimulation when parameters fall close to the recommended safety guidelines. Furthermore, EEG guidance of the TMS parameters can provide a means to optimize the timing of the TMS on the basis of the subject's temporary state of brain activity and thus maximize the achieved behavioral impact. **Figure 8** schematically summarizes a system for EEG-controlled TMS.

TMS and PET

PET can demonstrate changes in regional cerebral blood flow (rCBF) following TMS as initially shown by Paus et al. (106). PET offers the advantage of capturing cortical and subcortical activity simultaneously in the whole brain. One of the main technical difficulties faced in combining PET with TMS is the possible interference of the strong magnetic field of TMS with the photomultipliers of the gamma camera (sensitive to magnetic fields of approximately 10^{-4} T versus the nearly 2 T generated by TMS). To protect the gamma camera, Paus et al. shielded the photomultipliers with four layers of 0.5-mm-thick mu-metal. The homogenous thickness and density of

Figure 8

(*a*) TMS-induced amplifier saturation of EEG signal; (*b*) EEG signal; (*c*) combined TMS-EEG system.

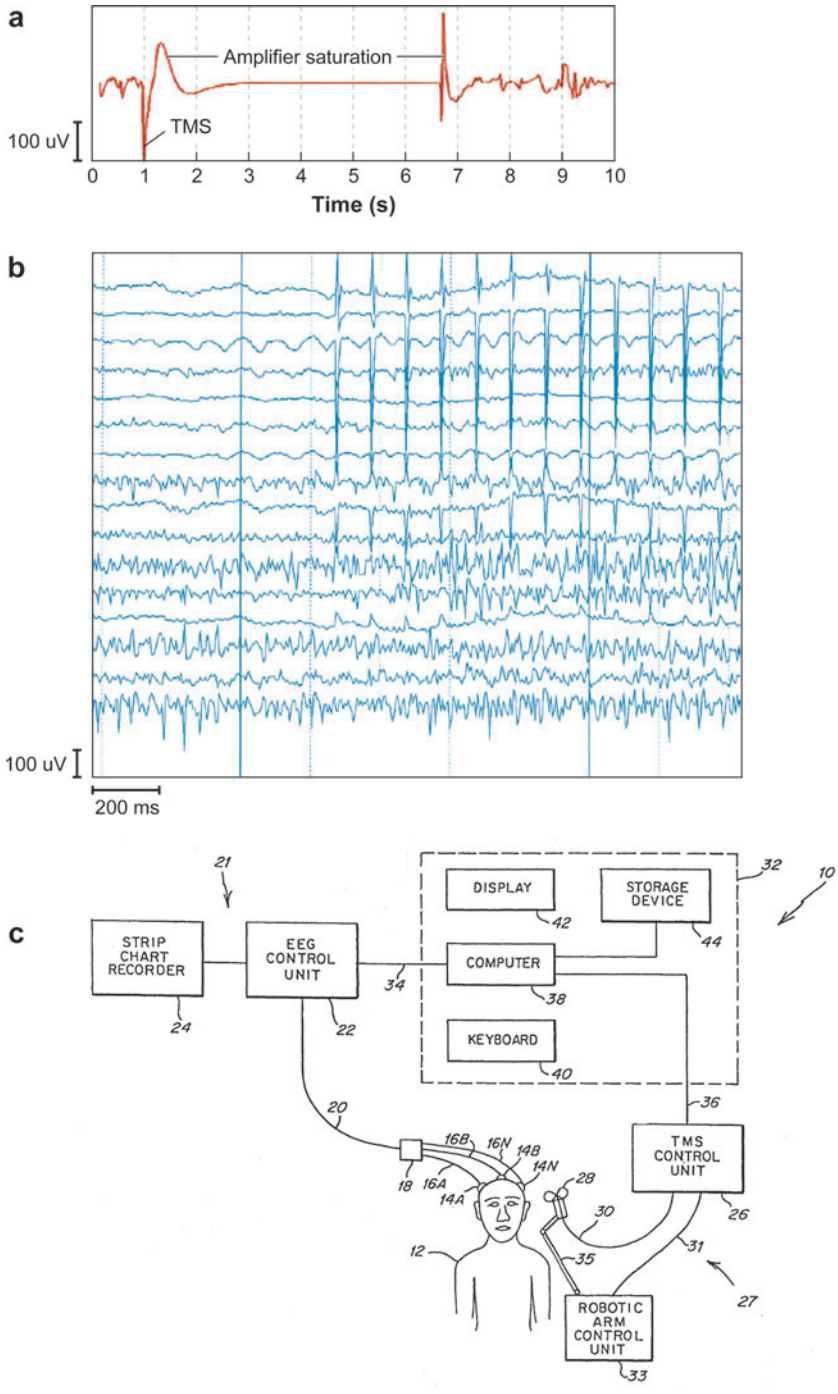

the shield is critical to prevent the appearance of artifacts in the images. However, the images are attenuated by approximately 22%, which might obscure some meaningful effects (100, 106, 107). In the meantime, the need for the use of a mu-metal shield has been challenged in other studies and it appears unnecessary (108, 109).

A number of authors have employed PET-TMS combinations to measure rCBF changes in response to TMS. Paus et al. (106) and Lee et al. (109) demonstrated a positive correlation between the number of TMS pulses and the rCBF changes in the targeted brain region as measured by PET. Siebner et al. studied the influence of different stimulation frequencies on rCBF (110). Negative correlations, suggestive of inhibitory effects of the stimulation, can be induced by specific patterns of rTMS (111) and network effects can be clearly demonstrated. For example, Speer et al. (112, 113) studied the effects of different stimulation intensities to prefrontal or motor cortex. In both studies, they demonstrated specific local changes in the targeted brain region and cortical and subcortical impact of selective neural structures. It is postulated that rCBF changes distal to the coil focus reflect functional connectivity and proximal changes reflect changes in cortical excitability.

As a measure of rCBF, the utility of PET may be limited. Regional CBF measures offer only indirect insights into neuronal impact of the stimulation. Furthermore, fMRI has a superior spatial resolution and allows for repeated, safe testing. However, FDG- and tracer-PET can provide unique insights into the metabolic effects of the stimulation and reveal direct physiologic information about mechanisms of action in the living human brain.

For example, Strafella et al. (114–116) pioneered the use of [^{11}C]-raclopride tracer PET to demonstrate changes in extracellular dopamine concentrations following rTMS. They extended this research to study the role of striatal dopamine release in Parkinsonian patients following TMS, demonstrating clear differences in the release between the symptomatic hemisphere and the asymptomatic hemisphere in the presymptomatic stage of Parkinsonian subjects (116). In addition to studies in Parkinson's disease, combined PET and TMS methodologies have been implemented, for example, in the study of depression (117), stroke (118, 119), or tinnitus (120). Tracer PET studies in such instances might be invaluable to guide therapeutic interventions and optimize stimulation parameters. For instance, in Parkinsonian patients, the dopamine differences between hemispheres could be used as a baseline to guide therapy and/or to monitor disease progression. Combined PET and TMS data can be utilized to generate network models and demonstrate the fundamental effects of brain stimulation on large-scale neural networks (121).

TMS and SPECT

Multiple single-photon emission computed tomography (SPECT) studies have been run in conjunction with TMS, where SPECT measurements are normally taken following administration of TMS to analyze rCBF, similar to the PET studies outlined above (122). In this fashion, SPECT is hampered by poorer spatial resolution than PET, but has the advantage of greater accessibility and lower cost. Importantly though, similar to the PET studies of Strafella et al., tracer-based SPECT systems

ROI: region-of-interest

have provided researchers with the ability to capture the impact of TMS on specific neurotransmitter systems. Pogarell et al. studied the use of IBZM SPECT as a means to study the effects of rTMS on dopaminergic neurotransmission by analyzing the degree of striatal IBZM binding to dopamine D2 receptors with a region-of-interest (ROI) technique (123). Other developments in this direction are surely desirable.

TMS and NIRS

Near infrared spectroscopy (NIRS) has allowed researchers to study brain hemoglobin levels in the coil region during and after TMS stimulation with temporal resolution (125 ms) second only to EEG, as has been demonstrated by Hada et al. (124) and Noguchi et al. (124a,b). Noguchi et al. extended the conventional NIRS technique by increasing the number of light emitter and detector pairs (a single pair is normally used in NIRS) that are capable of measuring optical changes in tissue brought about by hemoglobin concentration changes. They thus increased the signal-to-noise ratio of the technique such that it was capable of demonstrating both subthreshold and suprathreshold single-pulse TMS alterations in cortical oxyhemoglobin levels. Hada et al. (124) extended this technique to rTMS. As it is an optical technique, NIRS has the advantage of being relatively immune to any major electromagnetic artifact from the TMS and to allow the imaging of the cortical mantel, i.e., the main brain region of the TMS impact.

TMS and fMRI

Of all noninvasive imaging modalities, fMRI provides the clearest insight into the regions of the brain affected during TMS. In conjunction with TMS, fMRI provides better spatial resolution than EEG, SPECT, or PET and has a superior temporal resolution than all of the modalities except for EEG. Initially, researchers thought that limitations related to the synchronization of the fMRI slice acquisition with the TMS pulse and the signal noise caused by the TMS coil would be too difficult to overcome when combining the techniques. However, Bohning et al. (125–127) successfully imaged the blood oxygenation level-dependent (BOLD) signal during combined TMS and fMRI, and since this pioneering study, further improvements have been made that have focused on fMRI slice acquisition (orientation and timing), reduction of signal loss owing to the TMS coil, and removal of the artifacts caused by the TMS coil (128–134). Even with these improvements, there has still been great difficulty in resolving the BOLD signal directly under the TMS coil (for a review see Reference 131). Nevertheless, multimodal studies combining fMRI and TMS directed at visualizing the effects of TMS over the distributed cortex, between cortico-cortico connections, and cortico-subcortical connections have proven powerful and fruitful, and work continues on elucidating the BOLD signal in the TMS coil region (**Figure 9**).

tDCS

tDCS has been combined with EEG (135–137), PET (138), and fMRI (128). The technical challenges of combining tDCS with other techniques are less difficult to

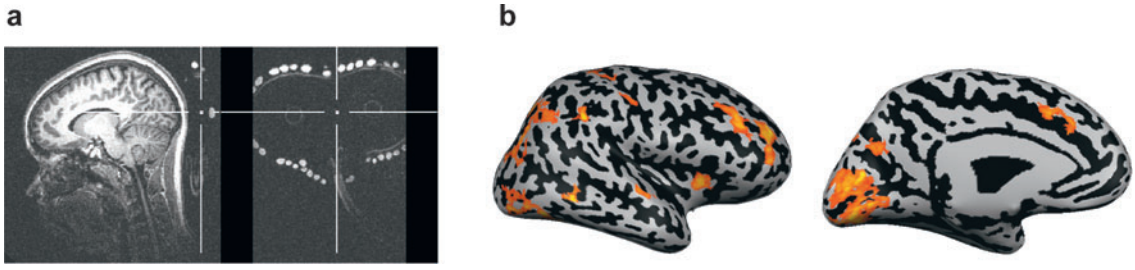

Figure 9

Depictions of fMRI and TMS, showing (*a*) anatomical MRI with coil representation, where the coil is centered above the primary visual cortex and in the inset the TMS coil is highlighted with vitamin E pills, and (*b*) fMRI BOLD activity evoked from single-pulse TMS on the primary visual cortex.

overcome than those of TMS, as no large stimulation artifact exists with tDCS. Ardolino et al. (135) studied the after-effects of tDCS (10 min, 1.5 mA cathodal stimulation to right motor cortex) on the EEG and found significant effects on the total power, delta, and theta activity, but statistically insignificant changes in the power of the alpha and beta/gamma rhythms with a two-way ANOVA analysis. They also assessed the affects of tDCS on spontaneous EEG activity, finding increased theta and delta rhythms indicative of large-scale network changes outside the region of the tDCS focus. Other researchers combined these modalities while studying sleep (136) and visual processes (137). Lang et al. (138) used PET to show widespread changes in rCBF in cortical and subcortical regions post tDCS (1 mA, 10 min), again indicative of the large-scale network changes brought about by tDCS. Baudewig et al. (128) studied the effects of tDCS on the fMRI BOLD signal both 5 and 15–20 min after a 5 min period of 1 mA stimulation. They found a significant increase in the mean number of activated pixels, which decayed with time following cathodal stimulation, while anodal stimulation accounted for a 5% nonsignificant change.

FUTURE DIRECTIONS AND CONCLUSIONS

Noninvasive brain stimulation has undergone a remarkable evolution since its inception. Today, scientists and physicians have the ability to explore the foundations of brain function and may ultimately alleviate numerous neuropsychiatric ailments with the controlled application of electromagnetic energy. The stimulator technology currently available has allowed the development of potentially more effective neuromodulatory patterns of stimulation (98, 139). Both TMS and tDCS have been coupled with imaging modalities (EEG, PET, fMRI, etc.), furthering our understanding of these stimulation techniques and providing clinicians with further means to assess neurological pathologies, reveal pathophysiology of disease, and understand mechanisms of action of brain stimulation. Nevertheless, even with all of these improvements, there are still many ongoing and future innovations that are necessary to take brain stimulation into the future.

DSI: diffusion spectrum imaging

MEG: magneto-encephalogram

The development of new and improved stimulator technology is an area of ongoing study and presents numerous challenges for biomedical and electrical engineers. In the area of TMS device design, advancements are continuously being made to increase the machine pulse frequencies. With ever increasing frequencies, problems related to coil heating become even more difficult to address; the current solutions implement air- or liquid-cooling mechanisms. However, it is possible that future developments could be implemented using TMS coils made of materials with lower specific heat, implementing novel heat sink strategies, or using gas-cooled TMS coil systems similar to modern MRI (however, such a system would be impractical with current technologies available).

There are many ongoing projects to improve on the current TMS tracking technology. To account for cortical current perturbations seen in neuropathologies that are not accounted for with conventional tracking systems, our group is integrating a tracking system with an FEM electromagnetic field solver based on individual patient MRIs, whereby the patient's anatomical MRI data and their tissue electromagnetic properties are mapped into the FEM mesh space. In practice, this technique will allow clinicians and researchers to predict the location, orientation, and magnitude of the induced stimulating current densities in individual patients based on individualized tissue heterogeneities, anisotropies, and dispersive properties. This control will allow one to ascertain the effects of pathological processes on TMS-induced current densities.

New imaging technologies are being developed that may eventually be fruitful to combine it in multimodal approaches with TMS or tDCS. For example, diffusion spectrum imaging (DSI) can provide critical insights into the conductivity of various brain tissues and can be used to improve the localization of EEG and magneto-encephalogram (MEG) sources. DSI provides information about fiber orientations in the white matter and the anisotropic conductivity of tissues. Thus, this technology could be used to investigate the orientation specificity of TMS and allow us to compare TMS with electromagnetic models of the brain that include interactions with neuronal subpopulations in gray matter and subcortical white matter resolved with DSI. This would allow one to test the potential neuroanatomic selectivity of TMS and assess the orientation-sensitivity of axonal reactivity to TMS, given the typical fanning orientations of subcortical white matter.

As knowledge of TMS effects on various pathologies is gained, devices have been proposed that are targeted for specific clinical implementation. Common to most therapeutic application of rTMS is the fact that stimulation has to be applied repeatedly for consecutive days (generally 10 to 20 days) in daily or even bidaily sessions. Under current methodology and practice, this means that patients have to go to the doctor's office or laboratory daily. It may also be better for rTMS treatment effectiveness to be delivered for a longer period of time or for short periods of time but more frequently. Therefore, self-delivery of rTMS by the patient in his home environment may be far more effective and certainly would provide a much more flexible and individualizable protocol. One may therefore envision modular, portable TMS devices that are capable of being fitted to the patient's own headshape, incorporate the TMS coils so as to target the desired brain region in the patient, and are controllable by

telecommunications channels to tailor treatment to individuals. Such a device could prove very useful in the long-term treatment regiments of TMS for such ailments as depression. Other portable devices have been proposed for more acute treatment regiments; for example, a portable hand-held TMS device for self-administered stimulation for migraine treatment is being tested. In the area of epilepsy treatment, delivery of the TMS pulse at the precise time following an epileptic spike is likely critical, and thus, high frequency of stimulation (>100 Hz) and EEG-triggering of the stimulation would seem desirable. For such a purpose, a stimulation coil system with built-in EEG monitoring capabilities and appropriate EEG-control circuitry would seem advantageous.

As tDCS has been rapidly growing over the past five years, numerous improvements have been proposed and certainly will be implemented in future studies. tDCS offers a low-cost, potentially high-impact option for various pathologies that could easily become mainstream in home use for neurorehabilitation and neuropsychiatric treatments. Device improvements have been proposed to develop integrated tracking systems with tDCS solvers to predict stimulation sites based on relative electrode schemes, to implement multipolar electrode schemes to increase focality, and to add levels of biofeedback and control via online EEG monitoring. As more clinical knowledge is obtained, devices could be designed for home use with patient-specific parameters programmed into the device (i.e., timing and current amplitude of treatment).

Finally, TMS and tDCS both suffer from limited focality. For TMS, increased focality has been explored with unique coil shapes, smaller coils, and conductive shields, as explained above. For tDCS, investigators have proposed multipolar electrode schemes to superimpose fields to achieve increased focality. In addition to the limited focality of both techniques, neither offers a means to stimulate the brain subcortically, without maximally stimulating the cortical surface. These limitations represent an area of open study for future biomedical engineers. In addition to providing motivation for the future development of current TMS and tDCS technologies, these limitations provide even further motivation in the development of new modalities for noninvasive stimulation. Acoustic (140–143), microwave (144), extremely low-frequency magnetic fields (145), and pseudo-invasive combined methods (146) have been explored with varied levels of success. The challenge of developing a noninvasive method for focal deep-brain stimulation remains an important and challenging focus of research.

DISCLOSURE STATEMENT

Dr. Pascual-Leone has previously received grant funding from Magnatism Corp. He also holds patents on TMS and MRI, and TMS and EEG combinations.

ACKNOWLEDGMENTS

The work on this article was partly supported by CIMIT and NIH grants K24 RR018875, RO1-EY12091, RO1-DC05672, RO1-NS 47754, RO1-NS 20068,

R01-EB 005047, RO1-NS47754, and RO3-EY014588. AV-C was supported by grants from La Caixa (Spain) and the Spanish Ministry of Education, Culture, and Sports (EX2002-041). Large parts of the work summarized in this article were conducted with the invaluable collaboration of M. Zahn and A. Grodzinski. We thank M. Thivierge for the expert administrative support.

LITERATURE CITED

1. Pascual-Leone A, Bartres-Faz D, Keenan JP. 1999. Transcranial magnetic stimulation: studying the brain-behavior relationship by induction of 'virtual lesions.' *Philos. Trans. R. Soc. London B Biol. Sci.* 354:1229–38
2. Priori A. 2003. Brain polarization in humans: a reappraisal of an old tool for prolonged noninvasive modulation of brain excitability. *Clin. Neurophysiol.* 114:589–95
3. Davey K, Riehl M. 2005. Designing transcranial magnetic stimulation systems. *IEEE Trans. Magnet.* 41:1142–48
4. Cohen LG, Roth BJ, Nilsson J, Dang N, Panizza M, et al. 1989. Effects of coil design on delivery of focal magnetic stimulation. Technical considerations. *Electroenceph. Clin. Neurophysiol.* 75:350–57
5. Cohen D, Cuffin BN. 1991. Developing a more focal magnetic stimulator. Part 1: some basic principles. *J. Clin. Neurophysiol.* 8:102–11
6. Hsu KH, Durand DM. 2001. A 3-D differential coil design for localized magnetic stimulation. *IEEE Trans. Biomed. Eng.* 48:1162–68
7. Carbunaru R, Durand DM. 2001. Toroidal coil models for transcutaneous magnetic stimulation of nerves. *IEEE Trans. Biomed. Eng.* 48:434–41
8. Kraus KH, Gugino LD, Levy WJ, Cadwell J, Roth BJ. 1993. The use of a cap-shaped coil for transcranial magnetic stimulation of the motor cortex. *J. Clin. Neurophysiol.* 10:353–62
9. Roth B, Maccabee P, Eberle L, Amassian V, Hallet M, et al. 1994. In vitro evaluation of a 4-leaf coil design for magnetic stimulation of peripheral nerve. *Electroenceph. Clin. Neurophysiol.* 93:68–74
10. Lin BC, Chen IH. 1998. Modified transcranial electromagnetic motor evoked potential obtained with train-of-four monitor for scoliosis surgery. *Acta Anaesthesiol. Sin.* 36:199–206
11. Lin V, Hsiao I, Dhaka V. 2000. Magnetic coil design considerations for functional magnetic stimulation. *IEEE Trans. Biomed. Eng.* 47:600–10
12. Hsiao I, Lin V. 2001. Improved coil design for functional magnetic stimulation of expiratory muscles. *IEEE Trans. Biomed. Eng.* 48:684–94
13. Roth Y, Zangen A, Hallett M. 2002. A coil design for transcranial magnetic stimulation of deep brain regions. *J. Clin. Neurophysiol.* 19:361–70
14. Zangen A, Roth Y, Voller B, Hallett M. 2005. Transcranial magnetic stimulation of deep brain regions: evidence for efficacy of the H-coil. *Clin. Neurophysiol.* 116:775–79
15. Heller L, Hulsteyn DB. 1992. Brain stimulation using electromagnetic sources: theoretical aspects. *Biophys. J.* 63:129–38

16. Kim DH, Georghiou GE, Won C. 2006. Improved field localization in transcranial magnetic stimulation of the brain with the utilization of a conductive shield plate in the stimulator. *IEEE Trans. Biomed. Eng.* 53:720–25
17. Davey KR, Riehl M. 2006. Suppressing the surface field during transcranial magnetic stimulation. *IEEE Trans. Biomed. Eng.* 53:190–94
18. Tay GCM, Battocletti J, Sances A Jr, Swiontek T, Kurakami C. 1989. Measurement of magnetically induced current density in saline and in vivo. Engineering in Medicine and Biology Society, 1989. Images of the Twenty-First Century. *Proc. Annu. Int. Conf. IEEE* 4:1167–68
19. Maccabee P, Eberle L, Amassian VE, Cracco RQ, Rudell A, Jayachandra M. 1990. Spatial distribution of the electric field induced in volume by round and figure '8' magnetic coils: relevance to activation of sensory nerve fibers. *Electroenceph. Clin. Neurophysiol.* 76:131–41
20. Yunokuchi K, Cohen D. 1991. Developing a more focal magnetic stimulator. Part 2: fabricating coils and measuring induced current distributions. *J. Clin. Neurophysiol.* 8:112–20
21. Yunokuchi K, Koyoshi R, Wang G, Yoshino T, Tamari Y, et al. 1999. *Estimation of focus of electric field in an inhomogenous medium exposed by pulsed magnetic field*. Presented at IEEE First Joint BMES/EConf MBS. Serv. Humanit. Adv. Technol., Atlanta
22. Tay GCM, Battocletti J, Sances A Jr, Swiontek T. 1991. *Mapping of current densities induced in vivo during magnetic stimulation*. Presented at Annu. Int. Conf. IEEE Eng. Med. Biol. Soc. Orlando, FL
23. Lisanby S. 1998. Intercerebral measurements of rTMS and ECS induced voltage in vivo. *Biol. Psychiatry* 43:100s
24. Lisanby SH, Belmaker RH. 2000. Animal models of the mechanisms of action of repetitive transcranial magnetic stimulation (RTMS): comparisons with electroconvulsive shock (ECS). *Depress. Anxiety* 12:178–87
25. Wagner T, Gangitano M, Romero R, Theoret H, Kobayashi M, et al. 2004. Intracranial measurement of current densities induced by transcranial magnetic stimulation in the human brain. *Neurosci. Lett.* 354:91–94
26. Ueno S, Tashiro T, Harada K. 1988. Localised stimulation of neural tissues in the brain by means of a paired configuration of time-varying magnetic fields. *J. Appl. Phys.* 64:5862–64
27. Tofts PS. 1990. The distribution of induced currents in magnetic stimulation of the nervous system. *Phys. Med. Biol.* 35:1119–28
28. Cerri G, De Leo R, Moglie F, Schiavoni A. 1995. An accurate 3-D model for magnetic stimulation of the brain cortex. *J. Med. Eng. Technol.* 19:7–16
29. Roth BJ, Cohen LG, Hallet M. 1991. The electric field induced during magnetic stimulation. *Electroenceph. Clin. Neurophysiol. Suppl.* 43:268–78
30. Roth BJ, Saypol JM, Hallett M, Cohen LG. 1991. A theoretical calculation of the electric field induced in the cortex during magnetic stimulation. *Electroenceph. Clin. Neurophysiol.* 81:47–56
31. Esselle K, Stuchly M. 1992. Neural stimulation with magnetic fields: analysis of induced electrical fields. *IEEE Trans. Biomed. Eng.* 39:693–700

32. Eaton H. 1992. Electric field induced in a spherical volume conductor from arbitrary coils: applications to magnetic stimulation and MEG. *Med. Biol. Eng. Comput.* 30(4):433–40
33. Scivill I, Barker AT, Freeston IL. 1996. Finite element modelling of magnetic stimulation of the spine. *Proc. Annu. Int. Conf. IEEE. Med. Biol. Soc. 18th*, pp. 393–94. Piscataway, NJ: IEEE
34. De Leo R, Cerri G, Balducci D, Moglie F, Scarpino O, Guidi M. 1992. Computer modelling of brain cortex excitation by magnetic field pulses. *J. Med. Eng. Technol.* 16:149–56
35. Mouchawar G, Nyenhuis J, Bourland J, Geddes LA, Schaefer D, Riehl M. 1993. Magnetic stimulation of excitable tissue: calculation of induced eddy currents with a three-dimensional finite-element model. *IEEE Trans. Magnet.* 29:3355–57
36. Nadeem M, Thorlin T, Gandhi O, Persson M. 2003. Computation of electric and magnetic stimulation in human head using the 3-D impedance method. *IEEE Trans. Biomed. Eng.* 50:900–7
37. Branston NM, Tofts PS. 1991. Analysis of the distribution of currents induced by magnetic field in a volume conductor. *Phys. Med. Biol.* 36:161–68
38. Liu R, Ueno S. 1998. Simulation of the influence of tissue inhomogeneity on nerve excitation elicited by magnetic stimulation. Engineering in Medicine and Biology Society. *Proc. 20th Annu. Int. Conf. IEEE* 6:2998–3000
39. Wagner TA, Zahn M, Grodzinsky AJ, Pascual-Leone A. 2004. Three-dimensional head model simulation of transcranial magnetic stimulation. *IEEE Trans. Biomed. Eng.* 51:1586–98
40. Lemon R. 2002. Basic physiology of TMS. In *Handbook of Transcranial Magneic Stimulation*, ed. A Pascual-Leone, N Davey, JC Rothwell, EM Wassermann, BK Puri, pp. 61–77. London: Arnold
41. Starzynski J, Sawicki B, Wincenciak S, Krawczyk A, Zyss T. 2002. Simulation of magnetic stimulation of the brain. *IEEE Trans. Magnet.* 38:1237–40
42. Miranda PC, Hallett M, Basser PJ. 2003. The electric field induced in the brain by magnetic stimulation: a 3-D finite-element analysis of the effect of tissue heterogeneity and anisotropy. *IEEE Trans. Biomed. Eng.* 50:1074–85
43. Dymond AM, Coger RW, Serafetinides EA. 1975. Intracerebral current levels in man during electrosleep therapy. *Biol. Psychiatry* 10:101–4
44. Wagner T, Fregni F, Fecteau S, Grodzinsky A, Zahn M, Pascual-Leone A. 2007. Transcranial direct current stimulation: a computer based human model study. *Neuroimage.* doi:10.1016/j.neuroimage.2007.01.027
45. Bindman LJ, Lippold OC, Redfearn JW. 1962. Long-lasting changes in the level of the electrical activity of the cerebral cortex produced by polarizing currents. *Nature* 196:584–85
46. Bindman LJ, Lippold OC, Redfearn JW. 1964. The action of brief polarizing currents on the cerebral cortex of the rat (1) during current flow and (2) in the production of long-lasting after-effects. *J. Physiol.* 172:369–82
47. Rush S, Driscoll DA. 1968. Current distribution in the brain from surface electrodes. *Anesth. Analg.* 47:717–23

48. Malmivuo J, Plonsey R. 1995. *Bioelectromagnetism*. Oxford/New York: Oxford Univ. Press
49. Nathan SS, Sinha SR, Gordon B, Lesser RP, Thakor NV. 1993. Determination of current density distributions generated by electrical stimulation of the human cerebral cortex. *Electroenceph. Clin. Neurophysiol.* 86:183–92
50. Li DL, Rath WT, Journee HL, Sclabassi RJ, Sun M. 2005. *Finite element analysis of transcranial electrical stimulation for intraoperative monitoring*. Presented at Bioeng. Conf. IEEE Annu. Northeast, 31st, Hoboken, NJ
51. Holdefer RN, Sadleir R, Russell MJ. 2006. Predicted current densities in the brain during transcranial electrical stimulation. *Clin. Neurophysiol.* 117:1388–97
52. Di Lazzaro V, Oliviero A, Pilato F, Saturno E, Dileone M, et al. 2004. The physiological basis of transcranial motor cortex stimulation in conscious humans. *Clin. Neurophysiol.* 115:255–66
53. Tehovnik EJ. 1996. Electrical stimulation of neural tissue to evoke behavioral responses. *J. Neurosci. Methods* 65:1–17
54. Purpura DP, McMurtry JG. 1965. Intracellular activities and evoked potential changes during polarization of motor cortex. *J. Neurophysiol.* 28:166–85
55. Yunokuchi K, Kato R, Yoshida H, Tamari Y, Saito M. 1998. *Study on the distributions of induced electric field in an inhomogeneous medium exposed a pulsed magnetic field*. Presented at Annu. Int. Conf. IEEE the Eng. Med. Biol. Soc. Hong Kong Sar, China
56. Liu R, Ueno S. 2000. Calculating the activating function of nerve excitation in inhomogeneous volume conductor during magnetic stimulation using the finite element method. *IEEE Trans. Magnet.* 36:1796–99
57. Wagner T, Fregni F, Eden U, Ramos-Estebanez C, Grodzinsky A, et al. 2006. Transcranial magnetic stimulation and stroke: a computer-based human model study. *Neuroimage* 30:857–70
58. Roth B, Basser P. 1990. A model of stimulation of a nerve fiber by electromagnetic induction. *IEEE Trans. Biomed. Eng.* 37:588–97
59. Basser PJ. 1994. Focal magnetic stimulation of an axon. *IEEE Trans. Biomed. Eng.* 41:601–6
60. Basser PJ, Roth BJ. 1991. Stimulation of a myelinated nerve axon by electromagnetic induction. *Med. Biol. Eng. Comput.* 29:261–68
61. Durand D, Bikson M. 2004. Control of neuronal activity by electrical fields: in vitro models of epilepsy. In *Deep Brain Stimulation and Epilepsy*, ed. H Luders, pp. 67–86. London: Taylor & Francis Group
62. Rattay F. 1989. Analysis of models for extracellular fiber stimulation. *IEEE Trans. Biomed. Eng.* 36:974–77
63. Rattay F, Resatz S, Lutter P, Minassian K, Jilge B, Dimitrijevic MR. 2003. Mechanisms of electrical stimulation with neural prostheses. *Neuromodulation* 6:42–56
64. Hodgkin AL, Huxley AF. 1952. A quantitative description of membrane current and its application to conduction and excitation in nerve. *J. Physiol.* 117:500–44

65. Nilsson J, Panizza M, Roth BJ, Basser PJ, Cohen LG, et al. 1992. Determining the site of stimulation during magnetic stimulation of a peripheral nerve. *Electroenceph. Clin. Neurophysiol.* 85:253–64
66. Maccabee P, Amassian V, Cracco R, Cadwell J. 1988. An analysis of peripheral motor nerve stimulation in humans using the magnetic coil. *Electroenceph. Clin. Neurophysiol.* 70:524–33
67. Nagarajan S, Durand DM. 1995. Analysis of magnetic stimulation of a concentric axon in a nerve bundle. *IEEE Trans. Biomed. Eng.* 42:926–33
68. Nagarajan S, Durand DM. 1996. A generalized cable equation for magnetic stimulation of axons. *IEEE Trans. Biomed. Eng.* 43:304–12
69. Nagarajan S, Durand DM, Ferguson AS, Warman EN. 1991. *Magnetic stimulation of finite neuronal structures*. Presented at Annu. Int. Conf. IEEE Eng. Med. Biol. Soc. Orlando, FL
70. Nagarajan S, Durand DM, Warman EN. 1993. Effects of induced electric fields on finite neuronal structures: a simulation study. *IEEE Trans. Biomed. Eng.* 40:1175–88
71. Kamitani Y, Bhalodia VM, Kubota Y, Shimojo S. 2001. A model of magnetic stimulation of neocortical neurons. *Neurocomputing* 38–40:697–703
72. Terzuolo CA, Bullock TH. 1956. Measurment of imposed voltage gradient adequate to modulate neuronal firing. *Proc. Natl. Acad. Sci. USA* 42:687–94
73. Bindman LJ, Lippold OC, Redfearn JW. 1963. Comparison of the effects on electrocortical activity of general body cooling of the surface of the brain. *Electroenceph. Clin. Neurophysiol.* 15:238–45
74. Ueno S, Lovsund P, Oberg PA. 1986. Effect of time varying magnetic fields on the action potential in lobster giant axon. *Med. Biol. Eng. Comput.* 24:521–26
75. Maccabee P, Amassian V, Eberle L, Cracco R. 1993. Magnetic coil stimulation of straight and bent amphibian and mammallian peripheral nerve in vitro: locus of excitation. *J. Physiol.* 460:201–19
76. McCarthy S, Haradem D. 1990. Induced current constraints and capacitive effects in inductive nerve stimulation. *IEEE Trans. Biomed. Eng.* 37:598–605
76a. Dissado LA. 1987. Ion transport through nerves and tissues. *Comments Mol. Cell. Biophys.* 4:143–69
77. Esser SK, Hill SL, Tononi G. 2005. Modeling the effects of transcranial magnetic stimulation on cortical circuits. *J. Neurophysiol.* 94:622–39
78. Valero-Cabre A, Rushmore R, Lomber SG, Payne BR, Pascual-Leone A. 2005. Impact of repetitive transcranial magnetic stimulation of the parietal cortex on metabolic brain activity: a 14C-2DG tracing study in the cat. *Exp. Brain Res.* 163:1–12
79. Sgro JA, Ghatak NR, Stanton PC, Emerson RG, Blair R. 1991. *Repetitive High Magnetic Field Stimulation: The Effect upon Rat Brain*. Amsterdam: Elsevier
80. Wang H, Wang X, Scheich H. 1996. LTD and LTP induced by transcranial magnetic stimulation in auditory cortex. *Neuroreport* 7:521–25
81. Ji RR, Schlaepfer TE, Aizenman CD, Epstein CM, Qiu D, et al. 1998. Repetitive transcranial magnetic stimulation activates specific regions in rat brain. *Proc. Natl. Acad. Sci. USA* 95:15635–40

82. Post A, Muller MB, Engelmann M, Keck ME. 1999. Repetitive transcranial magnetic stimulation in rats: evidence for a neuroprotective effect in vitro and in vivo. *Eur. J. Neurosci.* 11:3247–54
83. Keck ME, Sillaber I, Ebner K, Welt T, Toschi N, et al. 2000. Acute transcranial magnetic stimulation of frontal brain regions selectively modulates the release of vasopressin, biogenic amines and amino acids in the rat brain. *Eur. J. Neurosci.* 12:3713–20
84. Keck ME, Welt T, Post A, Muller MB, Toschi N, et al. 2001. Neuroendocrine and behavioral effects of repetitive transcranial magnetic stimulation in a psychopathological animal model are suggestive of antidepressant-like effects. *Neuropsychopharmacology* 24:337–49
85. Levkovitz Y, Marx J, Grisaru N, Segal M. 1999. Long-term effects of transcranial magnetic stimulation on hippocampal reactivity to afferent stimulation. *J. Neurosci.* 19:3198–203
86. Poirrier AL, Nyssen Y, Scholtes F, Multon S, Rinkin C, et al. 2004. Repetitive transcranial magnetic stimulation improves open field locomotor recovery after low but not high thoracic spinal cord compression-injury in adult rats. *J. Neurosci. Res.* 75:253–61
87. Moliadze V, Zhao Y, Eysel U, Funke K. 2003. Effect of transcranial magnetic stimulation on single-unit activity in the cat primary visual cortex. *J. Physiol.* 553:665–79
88. Moliadze V, Giannikopoulos D, Eysel UT, Funke K. 2005. Paired-pulse transcranial magnetic stimulation protocol applied to visual cortex of anaesthetized cat: effects on visually evoked single-unit activity. *J. Physiol.* 566:955–65
89. Valero-Cabre A, Rushmore RJ, Payne BR. 2006. Low frequency transcranial magnetic stimulation on the posterior parietal cortex induces visuotopically specific neglect-like syndrome. *Exp. Brain Res.* 172:14–21
90. Valero-Cabre A, Payne BR, Pascual-Leone A. 2007. Opposite impact on 14C-2-deoxiglucose brain metabolism following patterns of high and low frequency repetitive transcranial magnetic stimulation in the posterior parietal cortex. *Exp. Brain Res.* 176(4):603–15
91. Aydin-Abidin S, Moliadze V, Eysel UT, Funke K. 2006. Effects of repetitive TMS on visually evoked potentials and EEG in the anaesthetized cat: dependence on stimulus frequency and train duration. *J. Physiol.* 574:443–55
92. Hayashi T, Ohnishi T, Okabe S, Teramoto N, Nonaka Y, et al. 2004. Long-term effect of motor cortical repetitive transcranial magnetic stimulation. *Ann. Neurol.* 56:77–85
93. Liebetanz D, Fregni F, Monte-Silva KK, Oliveira MB, Amancio-dos-Santos A, et al. 2006. After-effects of transcranial direct current stimulation (tDCS) on cortical spreading depression. *Neurosci. Lett.* 398:85–90
94. Liebetanz D, Klinker F, Hering D, Koch R, Nitsche MA, et al. 2006. Anticonvulsant effects of transcranial direct-current stimulation (tDCS) in the rat cortical ramp model of focal epilepsy. *Epilepsia* 47:1216–24
95. Post A, Keck ME. 2001. Transcranial magnetic stimulation as a therapeutic tool in psychiatry: what do we know about the neurobiological mechanisms? *J. Psychiatr. Res.* 35:193–215

96. Luft AR, Kaelin-Lang A, Hauser TK, Cohen LG, Thakor NV, Hanley DF. 2001. Transcranial magnetic stimulation in the rat. *Exp. Brain Res.* 140:112–21
97. Iyer MB, Schleper N, Wassermann EM. 2003. Priming stimulation enhances the depressant effect of low-frequency repetitive transcranial magnetic stimulation. *J. Neurosci.* 23:10867–72
98. Huang YZ, Edwards MJ, Rounis E, Bhatia KP, Rothwell JC. 2005. Theta burst stimulation of the human motor cortex. *Neuron* 45:201–6
99. Lee L, Siebner HR, Rowe JB, Rizzo V, Rothwell JC, et al. 2003. Acute remapping within the motor system induced by low-frequency repetitive transcranial magnetic stimulation. *J. Neurosci.* 23:5308–18
100. Paus T. 1999. Imaging the brain before, during, and after transcranial magnetic stimulation. *Neuropsychologia* 37:219–24
101. Amassian VE, Cracco RQ. 1987. Human cerebral cortical responses to contralateral transcranial stimulation. *Neurosurgery* 20:148–55
102. Amassian V, Eberle L, Maccabee P, Cracco R. 1992. Modeling magnetic coil excitation of human cerebral cortex with a peripheral nerve immersed in a brain-shape volume conductor: the signicance of fiber bending in excitation. *Electroenceph. Clin. Neurophysiol.* 85:291–301
103. Cracco RQ, Amassian VE, Maccabee PJ, Cracco JB. 1999. Interconnections between cortical areas revealed by transcranial magnetic stimulation. *Electroenceph. Clin. Neurophysiol. Suppl.* 50:129–32
104. Thut G, Ives JR, Kampmann F, Pastor MA, Pascual-Leone A. 2005. A new device and protocol for combining TMS and online recordings of EEG and evoked potentials. *J. Neurosci. Methods* 141:207–17
105. Ives JR, Rotenberg A, Poma R, Thut G, Pascual-Leone A. 2006. Electroencephalographic recording during transcranial magnetic stimulation in humans and animals. *Clin. Neurophysiol.* 117(8):1870–75
106. Paus T, Jech R, Thompson CJ, Comeau R, Peters T, Evans AC. 1997. Transcranial magnetic stimulation during positron emission tomography: a new method for studying connectivity of the human cerebral cortex. *J. Neurosci.* 17:3178–84
107. Thompson CJ, Paus T, Clancy R. 1998. Magnetic shielding requirements for PET detectors during transcranial magnetic stimulation. *IEEE Trans. Med. Imaging* 45:1303–7
108. Fox P, Ingham R, George MS, Mayberg H, Ingham J, et al. 1997. Imaging human intracerebral connectivity by PET during TMS. *Neuroreport* 8:2787–91
109. Lee JS, Narayana S, Lancaster J, Jerabek P, Lee DS, Fox P. 2003. Positron emission tomography during transcranial magnetic stimulation does not require micrometal shielding. *Neuroimage* 19:1812–19
110. Siebner HR, Takano B, Peinemann A, Schwaiger M, Conrad B, Drzezga A. 2001. Continuous transcranial magnetic stimulation during positron emission tomography: a suitable tool for imaging regional excitability of the human cortex. *Neuroimage* 14:883–90
111. Paus T, Jech R, Thompson CJ, Comeau R, Peters T, Evans AC. 1998. Dose-dependent reduction of cerebral blood flow during rapid-rate transcranial magnetic stimulation of the human sensorimotor cortex. *J. Neurophysiol.* 79:1102–7

112. Speer AM, Willis MW, Herscovitch P, Daube-Witherspoon M, Shelton JR, et al. 2003. Intensity-dependent regional cerebral blood flow during 1-Hz repetitive transcranial magnetic stimulation (rTMS) in healthy volunteers studied with H215O positron emission tomography: I. Effects of primary motor cortex rTMS. *Biol. Psychiatry* 54:818–25
113. Speer AM, Willis MW, Herscovitch P, Daube-Witherspoon M, Shelton JR, et al. 2003. Intensity-dependent regional cerebral blood flow during 1-Hz repetitive transcranial magnetic stimulation (rTMS) in healthy volunteers studied with H215O positron emission tomography: II. Effects of prefrontal cortex rTMS. *Biol. Psychiatry* 54:826–32
114. Strafella AP, Paus T, Barrett J, Dagher A. 2001. Repetitive transcranial magnetic stimulation of the human prefrontal cortex induces dopamine release in the caudate nucleus. *J. Neurosci.* 21: RC157
115. Strafella AP, Paus T, Fraraccio M, Dagher A. 2003. Striatal dopamine release induced by repetitive transcranial magnetic stimulation of the human motor cortex. *Brain* 126:2609–15
116. Strafella AP, Ko JH, Grant J, Fraraccio M, Monchi O. 2005. Corticostriatal functional interactions in Parkinson's disease: a rTMS/[11C]raclopride PET study. *Eur. J. Neurosci.* 22:2946–52
117. Kuroda Y, Motohashi N, Ito H, Ito S, Takano A, et al. 2006. Effects of repetitive transcranial magnetic stimulation on [(11)C]raclopride binding and cognitive function in patients with depression. *J. Affect Disord.* 95(1–3):35–42
118. Gerloff C, Bushara K, Sailer A, Wassermann EM, Chen R, et al. 2006. Multimodal imaging of brain reorganization in motor areas of the contralesional hemisphere of well recovered patients after capsular stroke. *Brain* 129:791–808
119. Chouinard PA, Leonard G, Paus T. 2006. Changes in effective connectivity of the primary motor cortex in stroke patients after rehabilitative therapy. *Exp. Neurol.* 201(2):375–87
120. Plewnia C, Reimold M, Najib A, Brehm B, Reischl G, et al. 2006. Dose-dependent attenuation of auditory phantom perception (tinnitus) by PET-guided repetitive transcranial magnetic stimulation. *Hum. Brain Mapp.* 28(3):238–46
121. Husain FT, Nandipati G, Braun AR, Cohen LG, Tagamets MA, Horwitz B. 2002. Simulating transcranial magnetic stimulation during PET with a large-scale neural network model of the prefrontal cortex and the visual system. *Neuroimage* 15:58–73
122. Okabe S, Hanajima R, Ohnishi T, Nishikawa M, Imabayashi E, et al. 2003. Functional connectivity revealed by single-photon emission computed tomography (SPECT) during repetitive transcranial magnetic stimulation (rTMS) of the motor cortex. *Clin. Neurophysiol.* 114:450–57
123. Pogarell O, Koch W, Popperl G, Tatsch K, Jakob F, et al. 2006. Striatal dopamine release after prefrontal repetitive transcranial magnetic stimulation in major depression: preliminary results of a dynamic [123I] IBZM SPECT study. *J. Psychiatr. Res.* 40:307–14

124. Hada Y, Abo M, Kaminaga T, Mikami M. 2006. Detection of cerebral blood flow changes during repetitive transcranial magnetic stimulation by recording hemoglobin in the brain cortex, just beneath the stimulation coil, with near-infrared spectroscopy. *Neuroimage* 32:1226–30
124a. Noguchi Y, Takeuchi T, Sakai KL. 2002. Lateralized activation in the inferior frontal cortex during syntactic processing: event-related optical topography study. *Hum. Brain Mapp.* 17(2):89–99
124b. Noguchi Y, Watanabe E, Sakai KL. 2003. An event-related optical topography study of cortical activation induced by single-pulse transcranial magnetic stimulation. *Neuroimage* 19(1):156–62
125. Bohning DE, Pecheny AP, Epstein CM, Speer AM, Vincent DJ, et al. 1997. Mapping transcranial magnetic stimulation (TMS) fields in vivo with MRI. *Neuroreport* 8:2535–38
126. Bohning DE, Shastri A, McConnell KA, Nahas Z, Lorberbaum JP, et al. 1999. A combined TMS/fMRI study of intensity-dependent TMS over motor cortex. *Biol. Psychiatry* 45:385–94
127. Bohning DE, Shastri A, Nahas Z, Lorberbaum JP, Andersen SW, et al. 1998. Echoplanar BOLD fMRI of brain activation induced by concurrent transcranial magnetic stimulation. *Invest. Radiol.* 33:336–40
128. Baudewig J, Nitsche MA, Paulus W, Frahm J. 2001. Regional modulation of BOLD MRI responses to human sensorimotor activation by transcranial direct current stimulation. *Magn. Reson. Med.* 45:196–201
129. Baudewig J, Paulus W, Frahm J. 2000. Artifacts caused by transcranial magnetic stimulation coils and EEG electrodes in T(2)*-weighted echo-planar imaging. *Magn. Reson. Imaging* 18:479–84
130. Baudewig J, Siebner HR, Bestmann S, Tergau F, Tings T, et al. 2001. Functional MRI of cortical activations induced by transcranial magnetic stimulation (TMS). *Neuroreport* 12:3543–48
131. Siebner HR, Lee L, Bestmann S. 2003. Interleaving TMS with functional MRI: now that it is technically feasible how should it be used? *Clin. Neurophysiol.* 114:1997–99
132. Bestmann S, Baudewig J, Frahm J. 2003. On the synchronization of transcranial magnetic stimulation and functional echo-planar imaging. *J. Magn. Reson. Imaging* 17:309–16
133. Bestmann S, Baudewig J, Siebner HR, Rothwell JC, Frahm J. 2003. Is functional magnetic resonance imaging capable of mapping transcranial magnetic cortex stimulation? *Suppl. Clin. Neurophysiol.* 56:55–62
134. Bestmann S, Baudewig J, Siebner HR, Rothwell JC, Frahm J. 2004. Functional MRI of the immediate impact of transcranial magnetic stimulation on cortical and subcortical motor circuits. *Eur. J. Neurosci.* 19:1950–62
135. Ardolino G, Bossi B, Barbieri S, Priori A. 2005. Non-synaptic mechanisms underlie the after-effects of cathodal transcutaneous direct current stimulation of the human brain. *J. Physiol.* 568:653–63
136. Marshall L, Molle M, Hallschmid M, Born J. 2004. Transcranial direct current stimulation during sleep improves declarative memory. *J. Neurosci.* 24:9985–92

137. Antal A, Kincses TZ, Nitsche MA, Bartfai O, Paulus W. 2004. Excitability changes induced in the human primary visual cortex by transcranial direct current stimulation: direct electrophysiological evidence. *Invest. Ophthalmol. Vis. Sci.* 45:702–7
138. Lang N, Siebner HR, Ward NS, Lee L, Nitsche MA, et al. 2005. How does transcranial DC stimulation of the primary motor cortex alter regional neuronal activity in the human brain? *Eur. J. Neurosci.* 22:495–504
139. Paulus W. 2005. Toward establishing a therapeutic window for rTMS by theta burst stimulation. *Neuron* 45:181–83
140. Antropov GA. 1962. Changes in cardiac activity following mechanical stimulation of the brain. *Biull. Eksp. Biol. Med.* 54:18–21
141. Mihran RT, Barnes FS, Wachtel H. 1990. Transient modification of nerve excitability in vitro by single ultrasound pulses. *Biomed. Sci. Instrum.* 26:235–46
142. Gavrilov LR, Tsirulnikov EM, Davies IA. 1996. Application of focused ultrasound for the stimulation of neural structures. *Ultrasound Med. Biol.* 22:179–92
143. Fry WJ. 1958. Intense ultrasound in investigations of the central nervous system. *Adv. Biol. Med. Phys.* 6:281–348
144. McRee DI, Wachtel H. 1980. The effects of microwave radiation on the vitality of isolated frog sciatic nerves. *Radiat. Res.* 82(3):536–46
145. Shupak NM, Hensel JM, Cross-Mellor SK, Kavaliers M, Prato FS, Thomas AW. 2004. Analgesic and behavioral effects of a 100 microT specific pulsed extremely low frequency magnetic field on control and morphine treated CF-1 mice. *Neurosci. Lett.* 354(1):30–33
146. Fry WJ. 1968. Electrical stimulation of brain localized without probes–theoretical analysis of a proposed method. *J. Acoust. Soc. Am.* 44(4):919–31

Annual Review of Biomedical Engineering
Volume 9, 2007

Contents

Indexes

Errata

An online log of corrections to *Annual Review of Biomedical Engineering* chapters (if any, 1977 to the present) may be found at http://bioeng.annualreviews.org/